CrossMark

ORIGINAL ARTICLE

Groundwater flow and chemistry of the oases of Al Wahat, NE Libya

Nawal Alfarrah[1,2] · Abdelrahim Hweesh[3] · Marc van Camp[1] · Kristine Walraevens[1]

Abstract The quality and geochemistry of groundwater are significantly affected by the depositional environment of aquifer sediments. Miocene sediments in Al Wahat area (Jalu, Awjilah and Shakherah Oases) in the Libyan Desert at the north-east of the country have been deposited in fluvial marginal marine and marine environments. The purposes of this paper are to describe the areal distribution of the dominant water quality constituents, to identify the major hydro-geochemical processes that affect the quality of water and to evaluate the relations of sedimentary depositional environments and groundwater flow to the quality and geochemistry of water in aquifer sediments of Post-Eocene. This study is the first investigation in Al Wahat Oasis and also in the whole Sahara, which introduces the importance of considering the end members and the synsedimentary influence for the interpretation of the aquifer hydrochemistry. The area involved in this study is within the boundaries 28°N–30°N and 21°E–23°E. Eighteen wells are selected in the area, including eight piezometers, and ten samples were analysed from wells used for domestic and agricultural purposes. Results show high and significant increase in total dissolved solids, especially Na^+, Cl^-, SO_4^{2-} and NO_3^- compared with the previous years. The chemical results for the groundwater samples in Al Wahat are classified according to the Stuyfzand groundwater classification system; the water type is mostly brackish and brackish-saline NaCl in the downstream direction and fresh-brackish $NaHCO_3$ upstream. These water types indicate that groundwater chemistry is changed by cation exchange reactions during flushing of the diluted saline aquifer by freshwater from the south. The different stages of cation exchange produce a chromatographic sequence of groundwater types. These cation exchange reactions during the freshening process occur mainly in the intercalated clay, resulting in a Na^+ increase, and peaks of K^+ and Mg^{2+} in the aquifer. In the north, the synsedimentary marine influence on the groundwater is stronger and the abstraction for irrigation is higher. Upconing of deep saline water and anthropogenic pollution may contribute significantly to the aquifer water quality. Calcite equilibrium and gypsum dissolution are also important hydrochemical processes in the aquifer.

✉ Nawal Alfarrah
Nawalr2003@yahoo.com

Abdelrahim Hweesh
ahweesh@yahoo.co.uk

Marc van Camp
marc.vancamp@ugent.be

Kristine Walraevens
Kristine.Walraevens@ugent.be

1 Laboratory for Applied Geology and Hydrogeology, Ghent University, Krijgslaan 281 S8, 9000 Ghent, Belgium

2 Geology Department, Az Zawiyah University, Az Zawiyah, Libya

3 General Water Authority, Tripoli, Libya

Introduction

The Great Sahara of North Africa is known to have undergone major hydrological fluctuations and was vegetated at times in the past. During wet phases, the region presently occupied by the Sahara was green, contained

forests, grasslands, and permanent rivers and lakes. When the wet periods ended at about 5.5 ka, the Sahara was transformed into a hyperarid desert and its original surface and alluvium-filled valleys and lake basins were totally covered with windblown sand sheets and dune fields (De Menocal et al. 2000). According to Sonntag et al. (1978) (Sultan et al. 1997), the heavy isotope content of fossil Saharan groundwaters (>32,000 year B.P.) reflects precipitation from Atlantic air masses as they crossed the Sahara from west to east during wet Pleistocene periods.

Since 1950s interest has grown in the study of groundwater resources and quality in North Africa and the Sahara (e.g. Sonntag et al. 1978; Sultan et al. 1997; Mohamed and Zineb 2015). Despite the major investigations that have been carried out in many regions, up to now, the hydrochemistry of the Saharan aquifers was only interpreted in terms of chemical reactions (e.g. evapoconcentration and rock dominated dissolution). This study highlights a new insight into the investigations of the hydrochemistry of Saharan aquifers in relation to the palaeo-hydrogeology, considering the end members within the depositional environment, taking Al Wahat Oases as an example.

Geological environments may contain naturally occurring saline water resulting from the synsedimentary deposits within each geological setting. Natural, highly saline waters typically have Cl^- as the dominant anion and Na^+ as the dominant cation. Exceptions are waters associated with saline seep and some salt flats, which often have SO_4^{2-} as a major anion (Richter and Kreitler 1993).

It is well known that the displacement of sea water by freshwater in an aquifer is manifested by a $NaHCO_3$-type water (Foster 1950; Back 1966; Lawrence et al. 1976; Chapelle and Knobel 1983; Walraevens 1987; Beekman 1991; Stuyfzand 1993; Coetsiers and Walraevens 2006; Walraevens et al. 2007, 2015). The underlying process is cation exchange, whereby Ca^{2+} from fresh $CaHCO_3$-type water exchanges with Na^+ that is present in the salt water-equilibrated cation exchange complex of the aquifer. The cation composition of sea water is dominated by Na^+, and Na^+ is therefore the most important cation in the sea water-equilibrated exchange complex. Mg^{2+} and K^+ are also present at increased concentration compared with fresh $CaHCO_3$ water. Freshening of an aquifer requires removal of these increased concentrations. The displacement leads to a chromatographic sequence in which the excess cations are flushed in the order of increasing affinity, i.e. the most selected cation disappears last from the exchanger (Appelo 1994).

The displacement of interstitial salt water by freshwater in marine sediments results in a typical $NaHCO_3$-type water upstream of the fresh-salt or fresh-brackish water interface (Walraevens et al. 2007). In aquifers, the chromatographic pattern may be obscured by flow conditions in the aquifer (e.g. mixing of waters of different origin) which change the relative concentrations of the cations Ca^{2+}, Mg^{2+}, Na^+ and K^+ (Appelo 1994). So the chromatographic patterns are difficult to detect in actual conditions. But confirmation of this theory has been described in detritic aquifers in the USA (Aquia Aquifer in Maryland, Appelo 1994), Dutch and Flemish polders (Beekman 1991; Stuyfzand 1993; Walraevens et al. 2005) or marine sediments (alternating clayey and sandy layers) in Flanders, Belgium (Cardenal and Walraevens 1994; Walraevens and Cardenal 1994; Walraevens et al. 2007; Blaser et al. 2010).

Study area

The area involved in this study is located in a desert in the north-eastern part of Sirte Basin, which is located in the north central part of Libya and contains the main oil fields in the country. Figure 1 shows the location and topographic map of Al Wahat.

The study area covers about 6400 km^2 from Al Wahat region. Al Wahat towns are located in oases (Jalu, Awjilah and Shakherah) at about 250 km from the Gulf of Sirte in the Mediterranean Sea in the north-west and 625 km from Al Kufra to the south. The Awjilah Oasis lies about 30 km north-west of Jalu Oasis, and Shakherah is at about 30 km in the north. Each oasis consists of a small hill covered by date palm trees, surrounded by a plain of red sand. These three oases had a population of 31,537 inhabitants in 2006 (GWA 2006). The main economic activities in the area are agriculture and many inhabitants work for companies in the oil sector.

Petroleum exploration in the Sirte Basin has led to the delineation and development of groundwater as well as oil and gas reserves. Groundwater reserves extend to great depths in the basin, but water quality generally deteriorates with depth and distance northward (Faitouri and Sanford 2015). These groundwater reserves are a part of the regional Nubian (NAS) and the Post-Nubian (PNAS) aquifer systems. The PNAS occurs in Sirte Basin and at the north part of the Al Kufra Basin to the south overlying the NAS and is comprised of Tertiary continental deposits. The water in these aquifers was recharged during the late Pleistocene and early Holocene wet periods (e.g. Voss and Soliman 2014).

The NAS and PNAS in eastern Libya including Al Wahat region were studied by many authors, including Ball (1927), Sandford (1935), Ezzat (1959), Gabert et al. (1961), Pallas (1981), Wright et al. (1982), Ahmad (1983), Pim and Binsariti (1994), Pallas and Salem (2000), Gossel et al. (2004), Faitouri (2013), Voss and Soliman (2014) and Faitouri and Sanford (2015).

According to Wright et al. (1982), the NAS in the Sirte Basin is buried much deeper than in the Al Kufra Basin
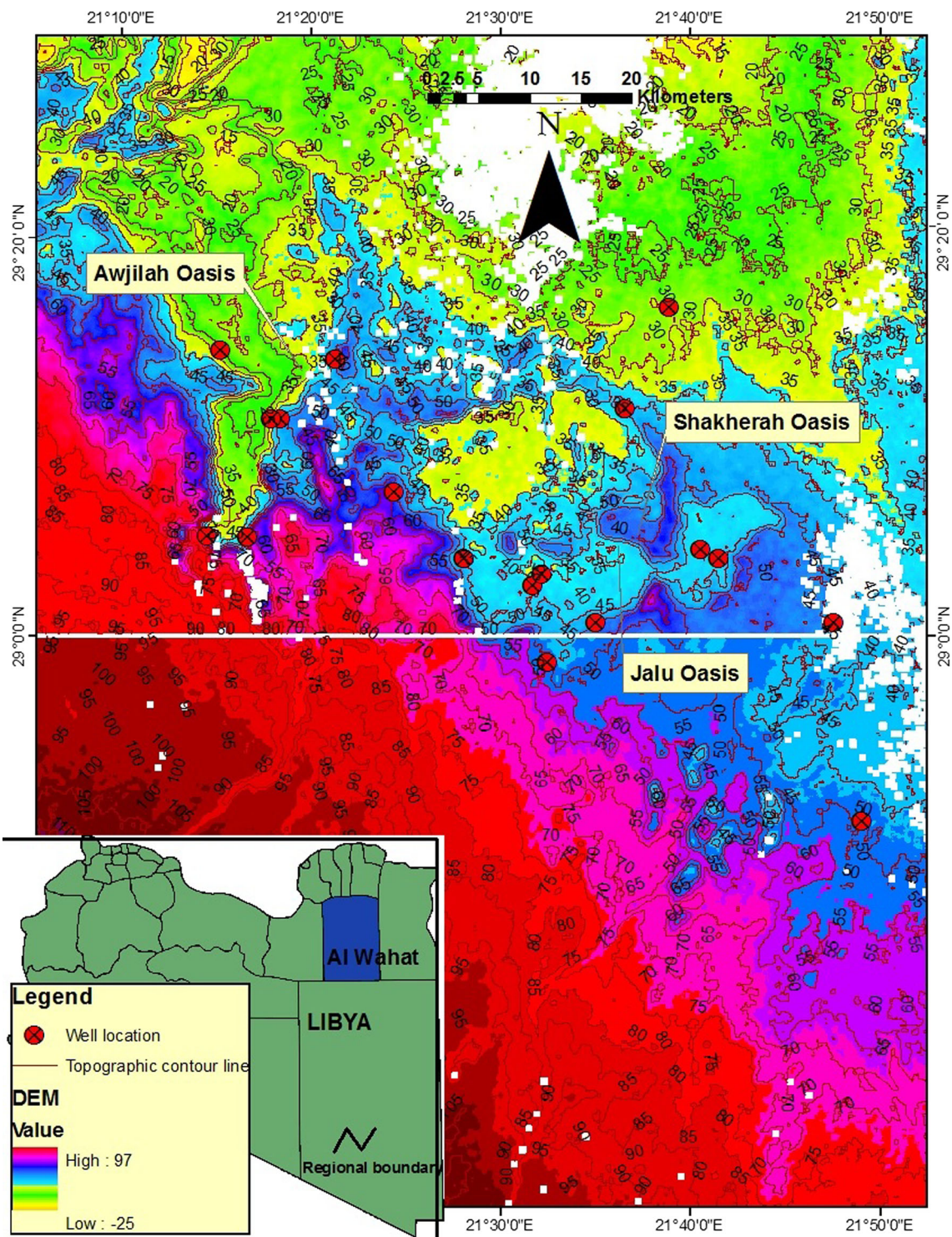
Fig. 1 Location map and topography of the study area. The *white colours in the map* are cells with no data

where it crops out at the surface. In Sirte Basin, the NAS is confined under artesian conditions. The quality of groundwater from the NAS in Sirte Basin including Al Wahat region is hypersaline; therefore, this study focuses on understanding the hydrochemistry of the Post-Nubian

Aquifer, which is the main aquifer in the region. The unconfined to semi-confined artesian Post-Nubian (or Post-Eocene) Aquifer in Al Wahat at the Libyan Desert is a multi-layered aquifer and was recharged in areas with higher topography at the south. This aquifer is mainly sand

and sandstone, with a series of fluviatile, medium- to coarse-grained sands with minor thicknesses of intercalated clay strata in the south-west, which grade into marine limestones, dolomites, evaporites, shales and clays with minor thicknesses of sandstones and sands in the north-east part. Initial conditions in these sediments were marine.

Marine conditions, with marine cations Na^+, K^+ and Mg^{2+} adsorbed onto clay minerals in these sediments before the last regression during Middle Miocene times, are being gradually expelled by infiltrating freshwater into the aquifer. Cation exchange processes by freshwater intrusion in detritial marine sediments have been observed in other areas, such as the Ledo-Paniselian aquifer in Flanders Belgium (Walraevens et al. 2007; Walraevens 1987, 1990), aquifers in coastal plains in the USA (Foster 1950; Back 1966; Chapelle and Knobel 1983; Appelo 1994), and in polder areas in The Netherlands (Appelo and Willemsen 1987; Beekman 1991; Stuyfzand 1993).

There are also local concerns, including excessive drawdown within pumping centres, contamination by polluted return flow water and disappearance of oases where most pumping centres are co-located, as well as the importance of this study is to evaluate the hydrochemical and hydrological condition of the aquifer and to show the control of cation exchange reactions on the groundwater chemistry of the aquifer in the region, where understanding the origin and mechanisms of the salinization process is essential for preventing further deterioration of groundwater resources in the study area.

Geology

Regional setting

Al Wahat geological setting is following the regional geology of Sirte Basin. Considerable information is available on the geology of Sirte Basin due largely to extensive oil exploration. The geological map for the eastern part of Libya including Sirte Basin is shown in Fig. 2 (after Wright et al. 1982).

The geological history of the Sirte Basin began in the late Precambrian by alternating periods of uplift and subsidence commencing with the Pan-African orogeny (Kroner 1993). The main structure of the Sirte Basin is the result of rifting, which formed the configuration of the basin. This began to develop in the Late Jurassic following a sequence of tectonic events that led to the breakup of the supercontinent Pangea (Gumati and Kanes 1985; Gumati and Nairn 1991; Van der Meer and Cloetingh 1993a, b; Baird et al. 1996; Schroter 1996). Uplift rises to 3000 m south of the Sirte Basin. Much of the land area in the basin, including Al Wahat region, is characterized by desert

steppes and includes aeolian deposits of the Calanscio Sand Sea of the Sahara Desert. Rifting originated in the Early Cretaceous, continued through Late Cretaceous and was completed by early Tertiary, resulting in a triple junction within the basin (Harding 1984; Gras and Thusu 1998; Ambrose 2000).

Stratigraphy

The Sirte Basin was initiated in Late Cretaceous times by collapse of the eroded Tibesti–Sirte uplift in the south. Subsidence continued but with decreasing intensity, possibly to Quaternary times (Wright and Edmunds 1971). Initially, the environment was mainly marine but with increasing lagoonal and continental facies developing in middle to late Tertiary. Early sediments were complex with deposition of shales in the grabens and carbonates on the horst blocks, but the later Cretaceous sedimentation became more uniformly argillaceous (Wright et al. 1982).

The Palaeozoic formations are mainly quartzitic sandstones and form thin residuals overlying the eroded basement areas but increase in thickness northwards. The Mesozoic continental sandstones range from the Upper Jurassic to Lower Cretaceous and have been subjected to several periods of erosion and chemical weathering. The overlying marine Upper Cretaceous comprises mostly shale which, in common with the later Tertiary formations, thickens towards the north–south axial zone of Sirte Basin.

The early Tertiary (Palaeocene and Eocene) formations are regionally extensive marine carbonates with subordinate shales, which present a marked lithological contrast to the underlying Mesozoic formations. During this time, the sea transgressed deep into the Tibesti embayment south of the basin and the Tertiary sediments exhibit overlap onto older Palaeozoic rocks (Elakkari 2005).

Table 1 shows a detailed description of the Post-Eocene which is of most interest in a hydrological context for Al Wahat area and known as Post-Nubian. Oligocene sediments are dominantly marine comprising calcareous sandstone with clays and carbonate which increase in importance northwards. The succeeding Marada Formation of Lower and Middle Miocene age shows a similar pattern of facies change. Sands of fluvial origin dominate to the south-west of the basin. To the north, individual sand bodies interfering with clays, commonly evaporitic, and carbonates, and representing deposition in transitional environments, ultimately change into marine carbonates and clays (Alfarrah et al. 2013). In both the Oligocene and Lower–Middle Miocene, lithology and thickness variations have been related to shoreline trends and locations of major zones of subsidence and linear trends of increasing sand input. A major regression took place in Middle Miocene times and the succeeding Calanscio Formation rests on a
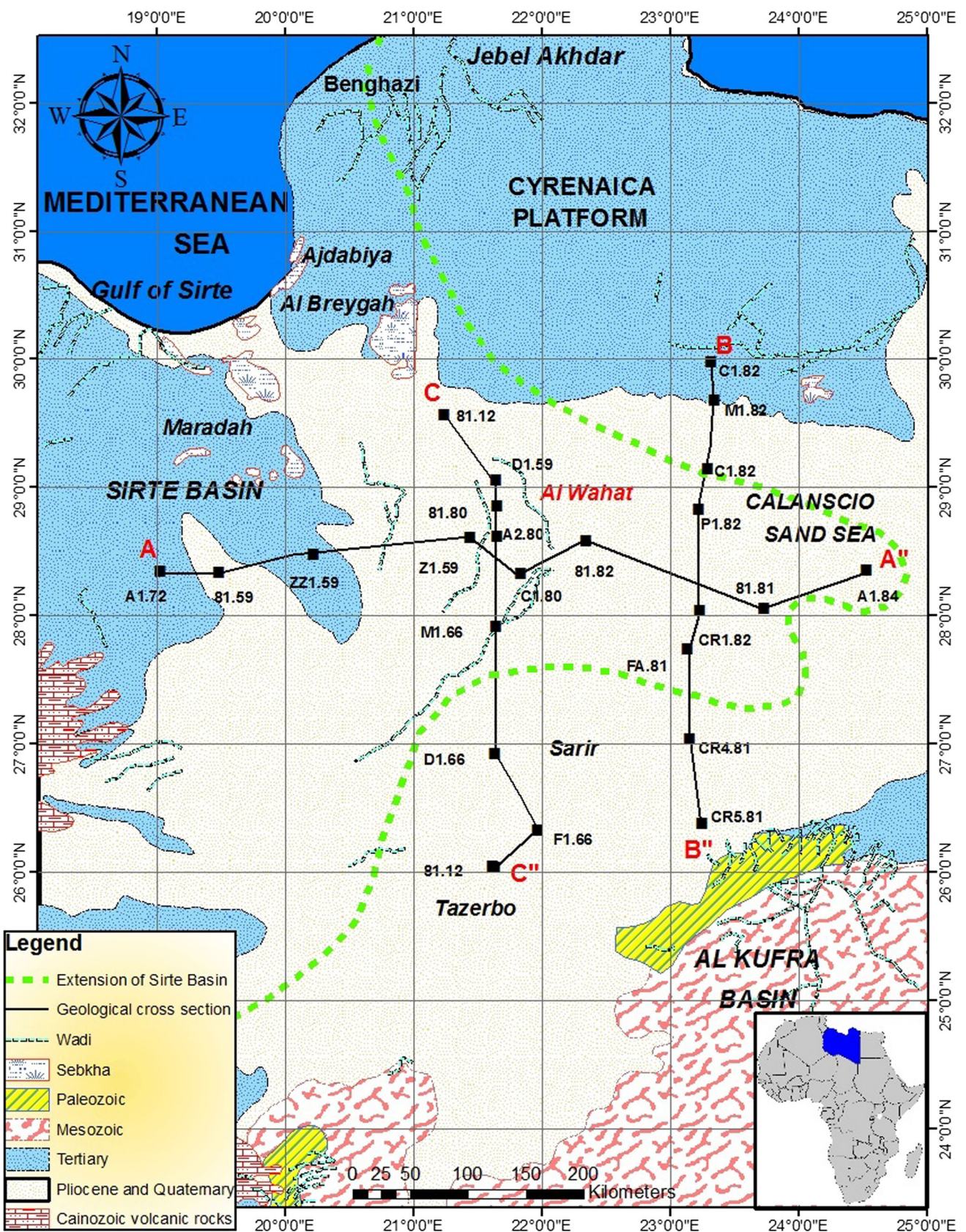
Fig. 2 Geological map for the NE Libya including Sirte Basin (after Wright et al. 1982)

Table 1 Description of the Post-Eocene deposits in Sirte Basin including Al Wahat area

Age	Formation name	Lithology and palaeo-environment	Thickness (m)
Holocene/Pleistocene	–	Surface sands, gravels and calcretes	0–30
Post-Middle Miocene (PMM)	Calanscio Formation	Medium- to coarse-grained sands, grading to calcareous sandstones, with thin clay interbeds	0–210
Lower and Middle Miocene (LMM)	Marada Formation	In the north marine carbonates and clays with evaporites; in the north-west: interbedded clays and marine carbonates; to south-east fluviatile sands and sandstone	121–697
Oligocene	–	Marine facies: glauconitic calcareous sandstones, limestones, dolomites and clays with some evaporites	242–730
		Non-marine facies: coarse-grained sand and sandstones with interbedded clay	

marked erosion surface. It comprises about 210 m of coarse sands with thin, intercalated clays. Significant thickness reduction in the Calanscio Formation is occurring northwards due to depositional change. Its age was determined as Post-Middle Miocene.

Hydrogeology

The important freshwater aquifers constituting regional groundwater systems in Libya occur within the Nubian Sandstone series of the Al Kufra Basin at the south (NAS) and the formations of Post-Eocene (PNAS) of Sirte Basin (Wright et al. 1982).

NAS consists of highly permeable continental sandstones containing layers of siltstones, shallow marine shales and clays of much lower hydraulic conductivity and unknown lateral continuity (Voss and Soliman 2014). The sandstone wedges out where crystalline Precambrian basement outcrops in the Uweinat Mountain at the south-eastern border. In the north-east, the Nubian aquifer dips northward, reaching an unknown extension below the Mediterranean Sea. In the south-east, the Nubian sandstones are unconfined; the northward dipping Nubian sandstones are overlain by stratified permeable continental deposits and low hydraulic conductivity shales and carbonates (Faitouri 2013).

The main occurrence of the Nubian Sandstone Aquifer is within the Al Kufra Basin. The whole sedimentary sequence of the Nubian Aquifer in the Al Kufra Basin is of Lower Devonian age, mainly consisting of marginal marine deposits of Tadrat Formation (Pim and Binsariti 1994). Aquitards lying above and beneath the main aquifers consist of shale, fine-grained argillaceous, ferruginous sandstones with mudstone interbeds (Pim and Binsariti 1994). Continental Mesozoic sandstones equivalent to the Nubian Sandstone extend beneath the Tertiary sequence of Sirte Basin (Wright et al. 1982). Figure 3 is a block diagram showing both systems (after Salem and Pallas 2002).

Post-Eocene or Post-Nubian (PNAS) is a very heterogeneous unconfined to semi-confined multi-aquifer system.

In Al Wahat region, it is mainly consisting of marginal fluvial and marine deposits of Post-Middle Miocene (PMM) Calanscio Formation and Lower–Middle Miocene (LMM) Marada Formation. Groundwater flow in the aquifer is effectively horizontal with negligible vertical hydraulic head differentials (Wright et al. 1982). Further north where clays and carbonates increase in amount, the deeper horizons become fully artesian and exhibit marked upward head gradients. The feature is attributed to restricted discharge in the less deeper horizons. The Oligocene layer has no important hydrologic context, due to high clay content and poor hydraulic characteristics and quality. The transmissivity of the Post-Eocene aquifer shows an increasing trend from south to north, from 600 to 1500 m^2/day (Wright et al. 1982) due to lithological change from fluvial to marine deposits.

The hydrological study of the Al Wahat area has begun in 1971, and the piezometric wells in the area were mostly drilled in 1973. Figure 4 shows the regional pre-pumping piezometric map for NE Libya in both Nubian and Post-Nubian aquifer systems. The contour lines were derived from the piezometric data in 1973 (Wright et al. 1982). The general direction of groundwater flow is south to north, where high hydraulic heads were found in the recharge areas in Sarir and near by Tazerbo (or Tazirbu) southwards and in Tebesti Mountain at the south border. The arrows indicate horizontal groundwater flow directions. Some of the flow from south to north in the NAS of the Al Kufra Basin may continue into the Sirte Basin in the north, but this is not clearly established. Wright et al. (1982) showed that the potentiometric surface in the northern part of the NAS in the Al Kufra Basin is somewhat continuous with the potentiometric surface in the PNAS, which may suggest a hydraulic connection across the basin boundaries. Figure 5 shows hydrological cross sections cut east–west and north–south through Sirte Basin including Al Wahat region; these cross sections are indicated in the geological map in Fig. 2. The aquifer contains freshwater at the south of the basin, becoming brackish to saline in the north, particularly in the deeper levels which have increasing

Fig. 3 Block diagram with the Nubian and Post-Nubian system NE Libya (after Salem and Pallas 2002)
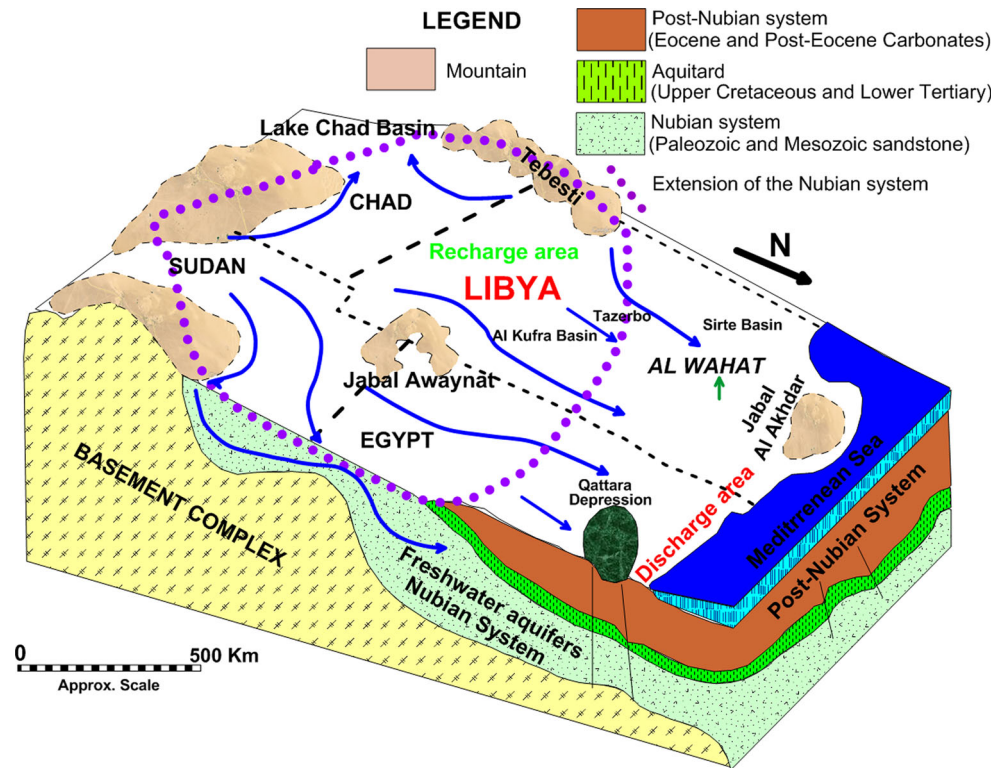
clay, carbonates and evaporites leading to high TDS. The water table is at or below sea level in the vicinity of the discharge area in the north and rises to about 200 m to the south of the basin. Hydrogeological information on underlying Eocene and Palaeocene indicates the presence of saline water and lower permeabilities in the mainly carbonate formations.

Some recharge by direct precipitation is very small or negligible, where the rainfall in the region is very low: it is in average 15 mm/year. Discharge occurs towards the Mediterranean Sea and low-lying sebkhas in the north and to a lesser extent in the scattered oases in the region. Nowadays, there are 600 palm farms in Al Wahat with 325 irrigation wells pumping from the Post-Eocene Aquifer, with pumped discharges amounting to 48 m^3/h per well and a total discharge of 37 Mm^3/year (Table 2). The aquifer storage coefficient is 0.1 (GWA 2014). Possible high runoff rates during the rainy season in high topographic areas suggest that the recharge from wadis could be important during humid years.

Methodology

Groundwater sampling and analysis

Quality data were collected from ten wells. This database is not quite extensive, but these are the only existing data in the database of General Water Authority and the wells are well distributed throughout the three oases to understand the origin and mechanisms of the hydrochemical processes in the area. The result of the analysis of 108 samples at Tazerbo around 500 km from Al Wahat in the upstream direction (Alfarrah et al. 2016) and one sample from areas in Sarir at 200 km towards the recharge area was also considered to evaluate the water quality along the flow path.

Ten water samples were retrieved from the database of the ministry of Libya, analysed by Libyan Petroleum Institute in 2013 by means of ICP-OES. These water samples were taken from drinking wells and irrigation wells with depths ranging from 100 to 200 m in Post-Middle Miocene Calanscio Formation (PMM). Four of these wells (S1, S2, S5 and S6) are used for domestic water supply, and the others are used for irrigation in farms and agricultural projects in the area. Physical and chemical parameters of groundwater from Al Wahat were measured: temperature (T), pH, electrical conductivity (EC), total hardness (TH), total hydrocarbons (TPH) and total dissolved solids (TDS). Samples were analysed for the major cations and anions (Na^+, K^+, Ca^{2+}, Mg^{2+}, SO_4^{2-}, Cl^-, HCO_3^-, CO_3^{2-} and NO_3^-). Trace elements As^{Total}, Cr^{Total}, Cu^{2+}, Hg^{2+}, Ni^{2+}, Pb^{2+} and Zn^{2+} were analysed.

Hydrochemical estimation methods

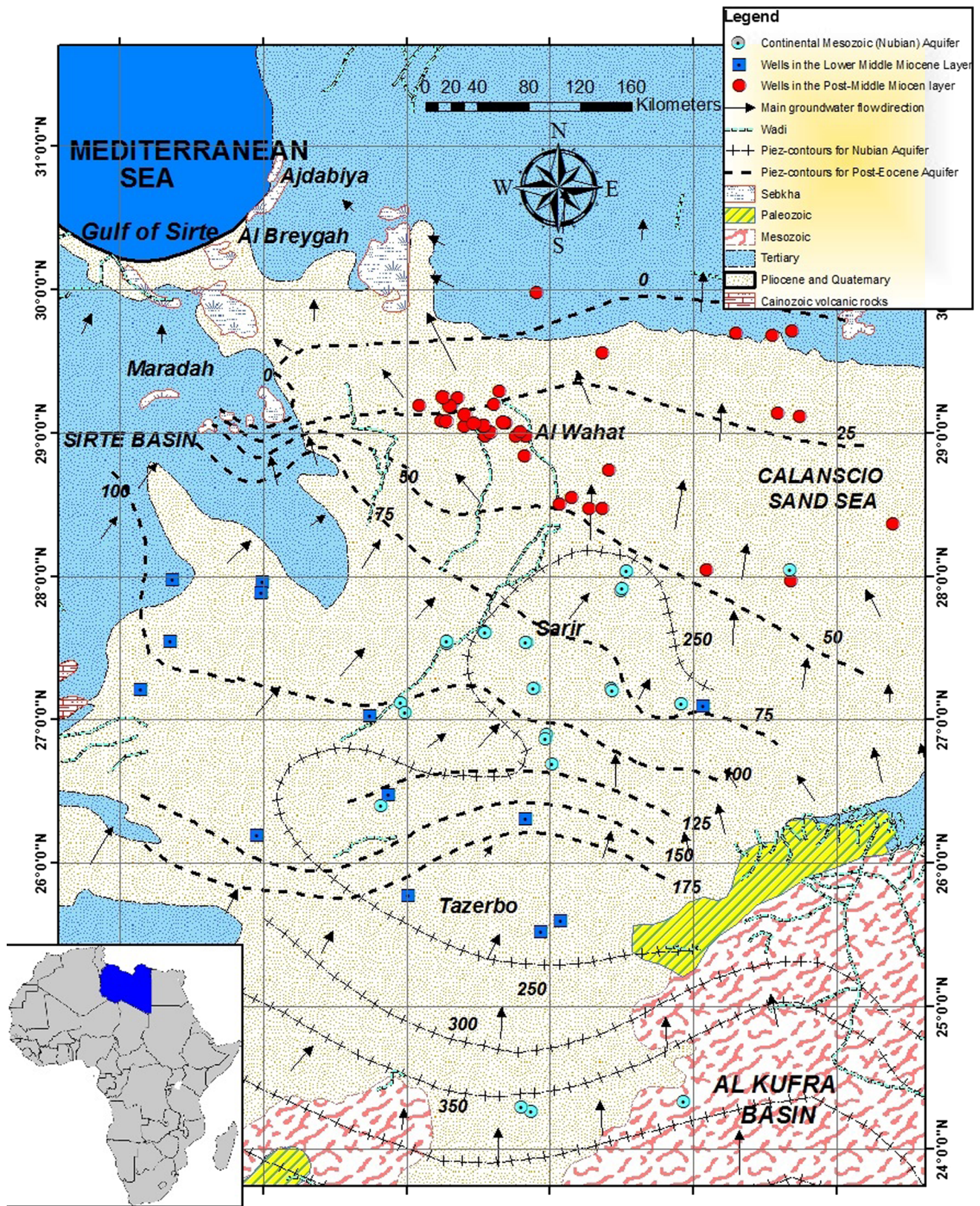The interpretation of analytical results was performed mainly based on the water-type classification according to

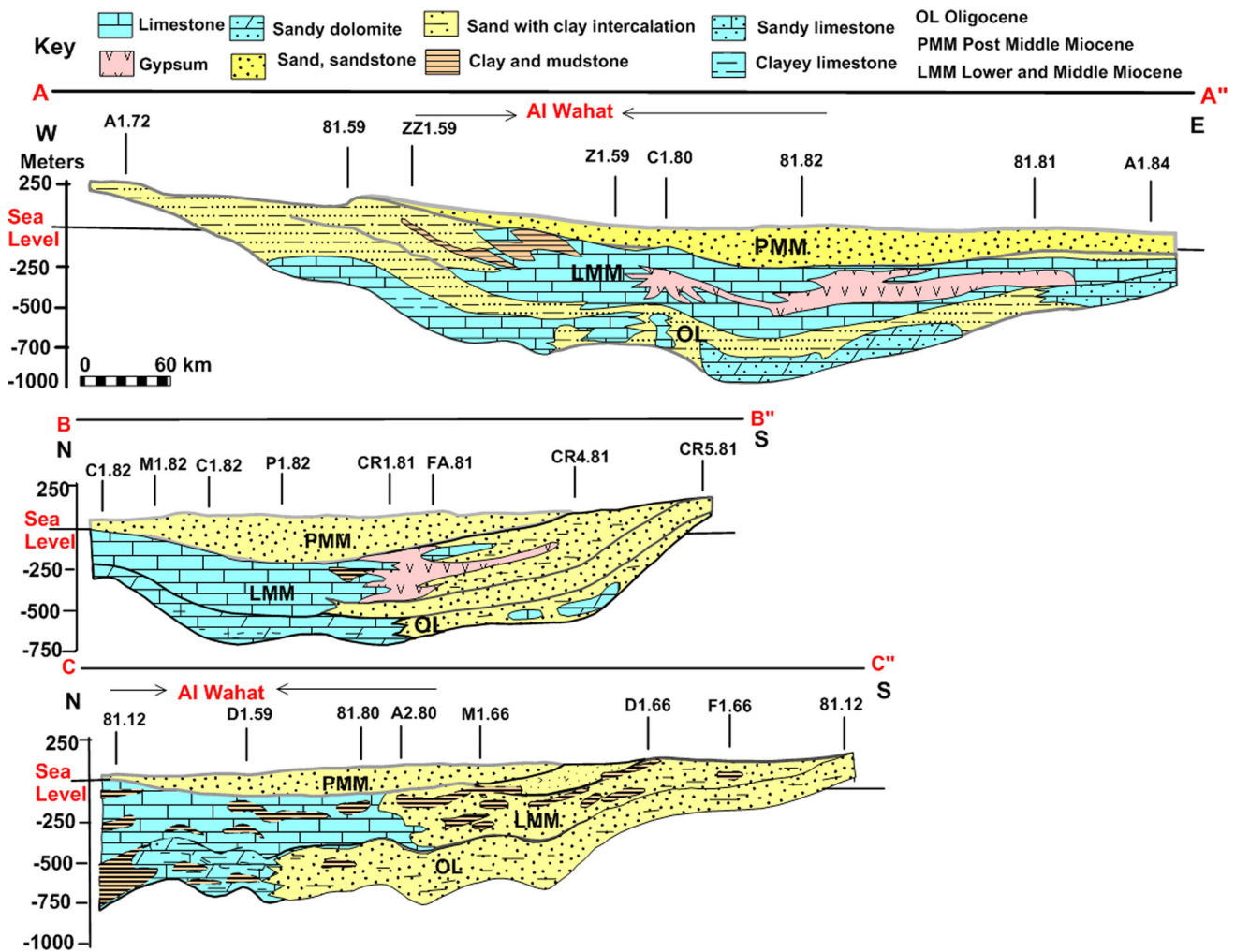**Fig. 4** Regional piezometric map for NE Libya including Al Wahat (around 1973)

Fig. 5 Hydrogeological cross sections for the Post-Eocene Aquifer in Sirte Basin (location in Fig. 2)

Table 2 Annual discharge from Al Wahat Data Palms Project (WDP) during period 2011–2014

No. of wells	Well discharge (Q) per well					Total discharge from all wells (m^3/irrigation year)
	m^3/h	Irrigation (h)	m^3/day	Irrigation period (days)	Irrigation (m^3/year)	
325	48	12	576	200	115,200	37,440,000

Stuyfzand (1986), saturation indices and ionic Δ calculation, graphical illustration methods including Piper diagram, calculation of ionic ratios cross-plots and elaboration of maps and cross sections showing the spatial and vertical distribution of water quality parameters in the study area.

Saturation indices and ionic Δ calculation

The PHREEQC 2.16 program (Parkhurst and Appelo 1999) for Windows was used to calculated saturation indices (SI) for calcite, dolomite, halite and gypsum based on the chemical analytical results and measured field temperatures for the ten samples. Positive values of SI indicate that the water is supersaturated with respect to the mineral phase (i.e. water will tend to precipitate the mineral), negative values indicate undersaturation (i.e. water which is in contact with the mineral will tend to dissolve it) and zero (or ±0.5) indicates equilibrium with the mineral.

Since equilibrium of solutes and minerals is not normally found, the saturation index only indicates in which direction the processes may go: for subsaturation dissolution is expected, and supersaturation suggests precipitation (Appelo and Postma 1993).

Calculation of the ionic deltas Δm_i (for SO_4^{2-}) consists of a comparison of the actual concentration of the constituent with its theoretical concentration for a freshwater/

sea water mix calculated from the Cl^- concentration of the sample (Fidelibus et al. 1993): Cl^- is dominant in sea water and can be assumed to be conservative in water (Appelo and Postma 1993). The chemical reactions during fresh/sea water displacement can be deduced by calculating a composition based on the conservative mixing of sea water and freshwater, and comparing the conservative concentrations with those in the samples. The mass fraction of sea water (f_{sea}) in the groundwater can be obtained from chloride concentrations of sea water and freshwater as follows (Appelo and Postma 1993; Yüce 2005):

$$f_{sea} = \frac{m_{Cl^-,sample} - m_{Cl^-,fresh}}{m_{Cl^-,sea} - m_{Cl^-,fresh}} \qquad (1)$$

where $m_{Cl^-,sample}$, the concentration of Cl^- in the sample expressed in mmol/l; $m_{Cl^-,fresh}$, the concentration of Cl^- in the freshwater expressed in mmol/l; $m_{Cl^-,sea}$, Cl^- concentration in the sea water end member in mmol/l ($Cl^- = 566$ mmol/l for mean ocean water; for Mediterranean Sea water (possible end member), $m_{Cl^-,sea} = 644.8$ mmol/l).

Based on the conservative mixing of sea water and freshwater, the concentration of an ion i (m_i) in the mixed waters was calculated using the mass fraction of sea water f_{sea} as follows (Appelo and Postma 1993):

$$m_{i,mix} = f_{sea} \cdot m_{i,sea} + (1 - f_{sea}) \cdot m_{i,fresh} \qquad (2)$$

where m_i is concentration of an ion i in mmol/l and subscripts mix, sea and fresh indicate the conservative mixture, and end members sea water and freshwater, respectively. Any change in concentration $m_{i,reaction}$ (Δm_i) as a result of reactions (not mixing) then becomes:

$$\Delta m_i = m_{i,reaction} = m_{i,sample} - m_{i,mix} \qquad (3)$$

where $m_{i,sample}$ = the actually observed concentration in the sample in mmol/l. Ions in freshwater near the coast are often derived from sea spray, and only Ca^{2+} and HCO_3^- are added due to calcite dissolution (Appelo and Postma 1993). In this case, $m_{i,fresh} = 0$ for all components except Ca^{2+} and HCO_3^-. If there is no other source for Cl^- and all of it is considered to be deriving from sea water, then f_{sea} can be written as:

$$f_{sea} = \frac{m_{Cl^-,sample}}{566} \qquad (4)$$

where Cl^- concentration is expressed in mmol/l and the Cl^- concentration of sea water is set at 566 mmol/l.

The main end members used in the calculations for this study are the Mediterranean Sea water and freshwater from the upper aquifer. For Mediterranean Sea water where $Cl^- = 644.8$ mmol/l, the sea water fraction is calculated as:

$$f_{sea} = \frac{m_{Cl^-,sample}}{644.8} \qquad (5)$$

The ion concentrations in the Mediterranean Sea water end member that was deposited with the aquifer are given in Table 2.

Cation exchange reactions in an aquifer: Stuyfzand classification

The Stuyfzand classification (Stuyfzand 1986, 1993) subdivides the most important chemical water characteristics at four levels. The primary type is determined based on the chloride content. The type is determined on the basis of an index for hardness. The classification into subtypes is determined based on the dominant cations and anions. Finally, the class is determined on the basis of the sum of Na^+, K^+ and Mg^{2+} in meq/l, corrected for a sea salt contribution. This classification is used to identify the evolution of chemical processes in groundwater.
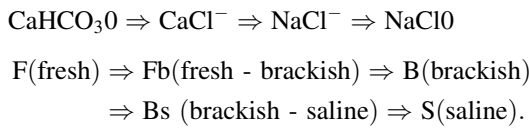
Walraevens and Van Camp (2005) explained the processes of freshening and salinization in aquifers with the end members sea water and freshwater. Freshwater is generally conceived as infiltrating rain having dissolved calcite, the water type is $F-CaHCO_30$, whereas sea water type is $S-NaCl0$ according to the classification of Stuyfzand (1986). The "0" in the class refers to the cation exchange equilibrium. This cation exchange code is based on the sign of:

$$(Na^+ + K^+ + Mg^{2+})_{corrected} = (Na^+ + K^+ + Mg^{2+})_{measured} - 1.061\, Cl^-\, (in\, meq/l).$$

A positive value greater than the error margin $\sqrt{0.50}\, Cl^-$ delivers "+" and refers to marine cation surplus, indicating freshening. A negative value ($<-\sqrt{0.50}\, Cl^-$) delivers "−": marine cation deficit pointing to salinization. A value in between both negative and positive error margin delivers "0": equilibrium. Salinization is induced as the new saline end member is introduced into the freshwater aquifer. The main chemical reaction is cation exchange, resulting in deficit of Na^+ and surplus of Ca^{2+}:

$$Na^+ + \frac{1}{2}Ca - X_2 \rightarrow Na - X + \frac{1}{2}Ca^{2+}$$
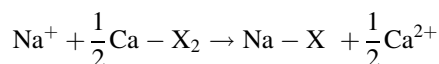
where X represents the natural exchanger in the reaction. During cation exchange, the dominant Na^+ ions are adsorbed and Ca^{2+} ions released, so that the resulting water moves from NaCl to CaCl water type, which is typical for salinization (Jones et al. 1999). The salinization process can be schematized as follows (Walraevens and Van Camp 2005):

$$CaHCO_30 \Rightarrow CaCl^- \Rightarrow NaCl^- \Rightarrow NaCl0$$

$$F(fresh) \Rightarrow Fb(fresh - brackish) \Rightarrow B(brackish)$$
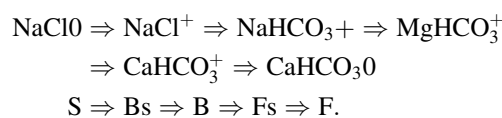$$\Rightarrow Bs\ (brackish - saline) \Rightarrow S(saline).$$

The chloride ion concentration is taken as a reference parameter (Jones et al. 1999). Therefore, as salt water intrudes coastal freshwater aquifers, the Na/Cl ratio decreases and the Ca/Cl ratio increases (Alfarrah 2011; Alfarrah et al. 2011).

Upon the inflow of freshwater in a saline aquifer, a reverse process takes place:

$$\frac{1}{2}Ca^{2+} + Na - X \rightarrow \frac{1}{2}Ca - X_2 + Na^+$$
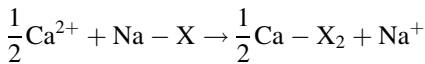
Flushing of the saline aquifer by freshwater will thus result in uptake of Ca^{2+} by the exchanger with concomitant release of Na^+. This is reflected in the increase in the Na/Cl ratio, and formation of the $NaHCO_3$ water type, which is typical for freshening. The anion HCO_3^- is not affected because natural sediments behave as cation exchanger at the usual near-natural pH of groundwater (Appelo 1994). The freshening process can be schematized as follows (Walraevens and Van Camp 2005):

$$NaCl0 \Rightarrow NaCl^+ \Rightarrow NaHCO_3+ \Rightarrow MgHCO_3^+$$
$$\Rightarrow CaHCO_3^+ \Rightarrow CaHCO_30$$
$$S \Rightarrow Bs \Rightarrow B \Rightarrow Fs \Rightarrow F.$$

Results and discussion

Hydraulic head variation

In general, the groundwater in Sirte Basin in Post-Nubian system flows northward towards the Mediterranean Sea and towards the scattered sebkha deposits.

Figure 6 shows a piezometric map for Al Wahat area, based on piezometric measurements of 18 wells in 2014. In general, this map agrees well with the topographic map in Fig. 1 and the piezometric observations in Fig. 4, taken at a time before groundwater flow was substantially influenced by pumping (around 1973). The general direction of groundwater flow is northwards to the main discharge area in the low-lying zone of sebkhas along the Gulf of Sirte. Other discharge areas of smaller significance are the scattered oases in the region.

However, the effect of local pumping can be seen in several wells in Awjilah and Shakherah, where low heads are observed. Figure 7 shows a water level and drawdown time series for 17 piezometers with measurement in 1973 (for four piezometers—the remaining wells were drilled after 2005) and 2010, 2013 and 2014 for all wells. It shows

that the drawdown is in the range of 12–25 m in 41 years (1973–2014) as a result of overabstraction from the aquifer.

Major hydrochemical parameters

Table 3 shows descriptive statistics for physico-chemical parameters of groundwater in the Al Wahat area. The results show that temperature ranges between 18 and 23 °C, pH range is 6.77–7.99, conductivity varies between 1798 and 10,320 μS/cm (25 °C), TDS range is 1439–7065 mg/l and chloride concentration ranges from 240 to 2699 mg/l.

Hydrochemical analysis shows that cation sodium (Na^+) is most abundant in the groundwater of Al Wahat with concentrations up to 1860 mg/l, while the most abundant anion is Cl^-, concentrations increasing up to 2699 mg/l for well S3 that pumps for a palm project at 10 km south of Shakherah Oasis. Sulphate is the second abundant anion present in high concentrations up to 1878 mg/l towards the north at well S4, which pumps for irrigation in Shakherah Oasis and well S5 in Jalu Oasis.

Figure 8a shows a contour map with the spatial distribution of Cl^- in Al Wahat for the analysed samples. High concentrations of chloride occur in wells at the north in mainly all samples in Shakherah Oasis and sample S5 in Jalu just to the south of Shakherah, where the concentrations are more than 2000 mg/l. More than 1000 mg/l of Cl^- is observed in Jalu Oasis for sample S6 and in Awjilah Oasis for all samples (i.e. S7, S8 and S9). The concentration of Cl^- decreases gradually towards the south, where it is only 240 and 260 mg/l at the south of the oases (in wells S1 and S2). The high Cl^- concentration is due to the effect of marine origin of the aquifer sediments (mainly the lower layer) and upconing of deep saline water due to pumping, which may also contribute significantly to the high salinity in the region.

Figure 8b shows the spatial distribution of SO_4^{2-} for the 10 samples in Al Wahat. Sulphate concentrations in the study area range from 244 mg/l to the south-east of Jalu to 1878 mg/l in the north at Shakherah Oasis. The highest concentrations in SO_4^{2-} with more than 1000 mg/l were recorded in Shakherah Oasis northwards for sample S4 and to the south of Shakherah in Jalu for sample S5. More than 600 mg/l SO_4^{2-} is observed for all samples in Awjilah Oasis. All samples in the area show SO_4^{2-} concentrations higher than the highest desirable level of 200 mg/l of the WHO (2008) standard. Synsedimentary marine influence could raise the SO_4^{2-} concentration for these waters together with mixing resulting from the upconing of the deep saline end member with high SO_4^{2-} concentrations.

In Fig. 8b, the SO_4^{2-} concentration distribution follows the same pattern as Cl^- concentrations in Fig. 8a,

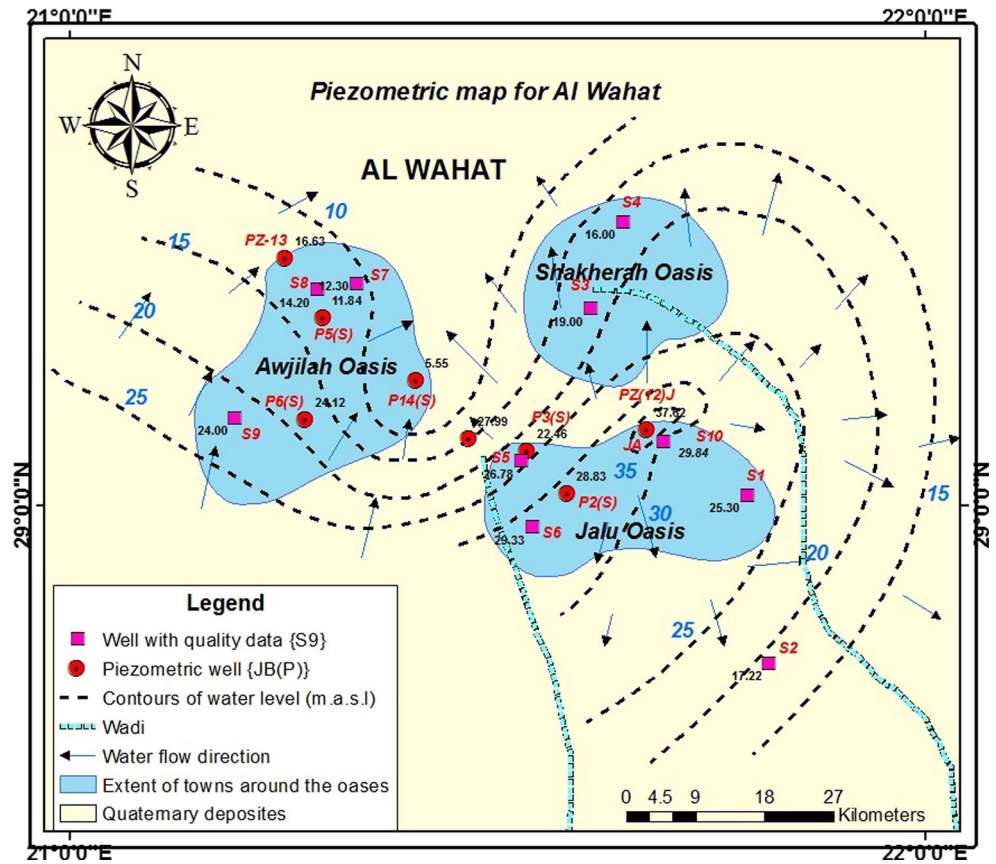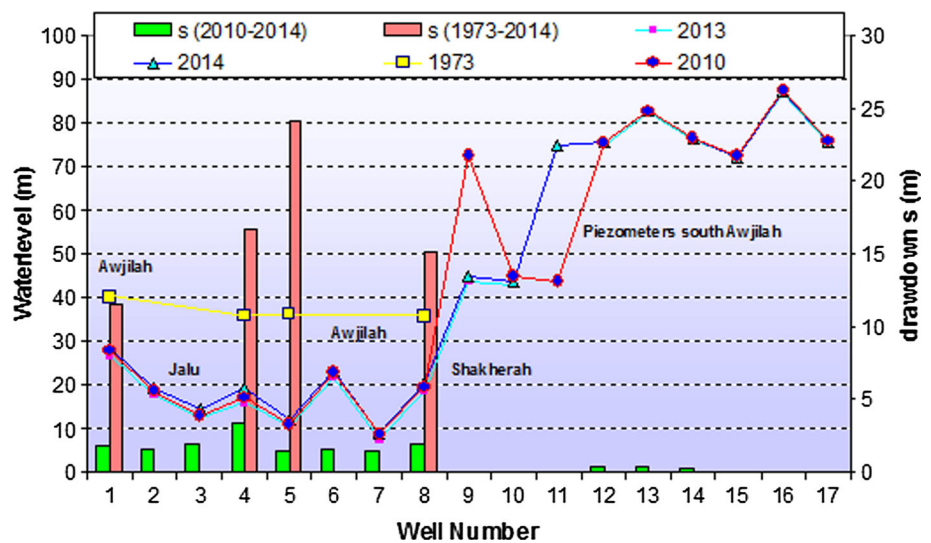**Fig. 6** Piezometric map for Al Wahat area

Fig. 7 Water level time series and drawdown in Al Wahat

where SO_4^{2-} is clearly linked to the high Cl^- concentration due to the marine influence of the aquifer and upconing of deep saline water as a result of overabstraction rates from the aquifer for irrigation at the north and west of the area in Shakherah and Awjilah Oases. The lower part of Lower–Middle Miocene age (Marada Formation) of the main aquifer is mainly carbonate and intercalated evaporites increase in amount northwards;

therefore, gypsum dissolution is another important hydrochemical process in the groundwater and contributes significantly to the high content of SO_4^{2-}. This has been further approved by the calculation of ΔSO_4^{2-} (Fig. 9), where higher values of ΔSO_4^{2-} than the mixture of sea water/freshwater are recorded for many samples. In general, all samples show positive ΔSO_4^{2-}. The gypsum dissolution from the lower part of the aquifer increases

Table 3 Descriptive statistics for physico-chemical parameters of groundwater (in mg/l) in the Al Wahat area

Parameters	Min	Max	Parameters	Min	Max
Na^+ (mg/l)	320	1860	TPH (mg/l)	<0.1 (detection limit 0.1)	
K^+ (mg/l)	8	35	pH	6.77	7.99
Ca^{2+} (mg/l)	59	480	TH	360	2601
Mg^{2+} (mg/l)	38	336	As^{Total} (ppm)	<0.02	
Cl^- (mg/l)	240	2699	Cd^{2+} (ppm)	<0.01	
SO_4^{2-} (mg/l)	244	1878	Cr^{Total} (ppm)	<0.002	
HCO_3^- (mg/l)	96	495	Cu^{2+} (ppm)	<0.002	
NO_3^- (mg/l)	8	199	Hg^{2+} (ppm)	<0.005	
TDS (mg/l)	1439	7065	Ni^{2+} (ppm)	<0.01	
EC (μS/cm 25 °C)	1798	10,320	Pb^{2+} (ppm)	<0.03	
T (°C)	18	23	Zn^{2+} (ppm)	<0.001	

ΔSO_4^{2-} to high positive values up to 20 mmol/l in sample S4.

Besides, the high SO_4^{2-} could be due to the evaporation of highly concentrated infiltrated water, where sebkha deposits are scattered at a few kilometres in the north and north-west of Al Wahat. High NO_3^- is recorded for some wells with high SO_4^{2-} and Cl^- concentrations, Fig. 10 shows spatial distribution of concentrations of NO_3^- in the study area. Nitrate levels for groundwater vary from 8 to 199 mg/l, the highest was recorded for well S5, which might relate to the fertilizers used in the Palm Project, and infiltration of highly polluted irrigation water might be due to high abstraction from the well.

Therefore, irrigation wells revealed that suffering from nitrate contamination caused an increase in the chance of nitrate pollution. Concentrations of more than 100 mg/l are recorded for many wells in the oases, and higher values than the desirable level of WHO (50 mg/l) were recorded for almost all samples in the region. High NO_3^- concentrations in these waters are a result of intensive agricultural activities in the area as well as pollution from surrounding cesspits due to lack of sewage system in the area.

Figure 11 shows the spatial distribution of electrical conductivity [EC μS/cm (25 °C)] in the study area. The spatial distribution of EC over the study area coincides with Cl^- distribution in Fig. 8a. The EC increases to about 10,320 μS/cm (25 °C) at the north and is higher than 1000 μS/cm (25 °C) for the whole sampled region.

In general, the TDS follows the same pattern as the EC, where saline water has been observed in the majority of wells in the study area, with TDS mostly over 1400 mg/l, which falls far above the highest desirable value of 500 mg/l for safe drinking water (WHO 2008). Drinking water supplies with TDS levels greater than the WHO maximum desirable level of 1500 mg/l are unpalatable to most consumers.

TDS and EC of groundwater salinity of Post-Eocene values indicate a large range of variation. It shows a strong mineralization of the water in the central and north direction of the study area. The water salinity in this area increases from south to north, which is illustrating existence of recharge processes at the southern part of the area. In other words, low TDS values, characterizing the southern and south-eastern border of the study area, reveal the dilution of the groundwater by the recharge coming from the southern border of this region. Beside the effect of the marine origin of sediment, gradual increase in groundwater salinity is also related to dissolution of evaporitic deposits in the lower aquifer layer.

The concentrations of trace elements such as As^{Total}, Zn^{2+}, Pb^{2+}, Cu^{2+}, Cd^{2+}, Ni^{2+} and Cr^{Total} are low and within the WHO ranges for all samples indicating the absence of groundwater contamination by these elements.

End members in the region

Recharge water in the area is the water flowing into the aquifer from the high topographic area in the south. Table 4 shows the ion concentrations in Mediterranean Sea water representing the marine end member that was deposited together with the aquifer, and samples from the south towards the recharge area in Sarir at about 200 km south of Al Wahat and in Tazerbo at about 500 km.

The recharge water in sample SE1 (Sarir) has a high concentration of Na^+, Ca^{2+} and HCO_3^-, and the water according to Stuyfzand classification is $NaHCO_3$ type as a result of calcite dissolution and cation exchange reaction during flushing of the aquifer by freshwater from the south. The analysed recharge water in Tazerbo (sample W101 with the lowest mineralization was selected out of 108 samples showing similar composition) is showing considerable concentrations of Mg^{2+}, Ca^{2+}, Na^+ and HCO_3^-, and according to Stuyfzand, the water is $MgHCO_3$ type, as a result of carbonate dissolution and the impact of cation exchange reactions during freshening of the aquifer, which is characteristic for the study area.
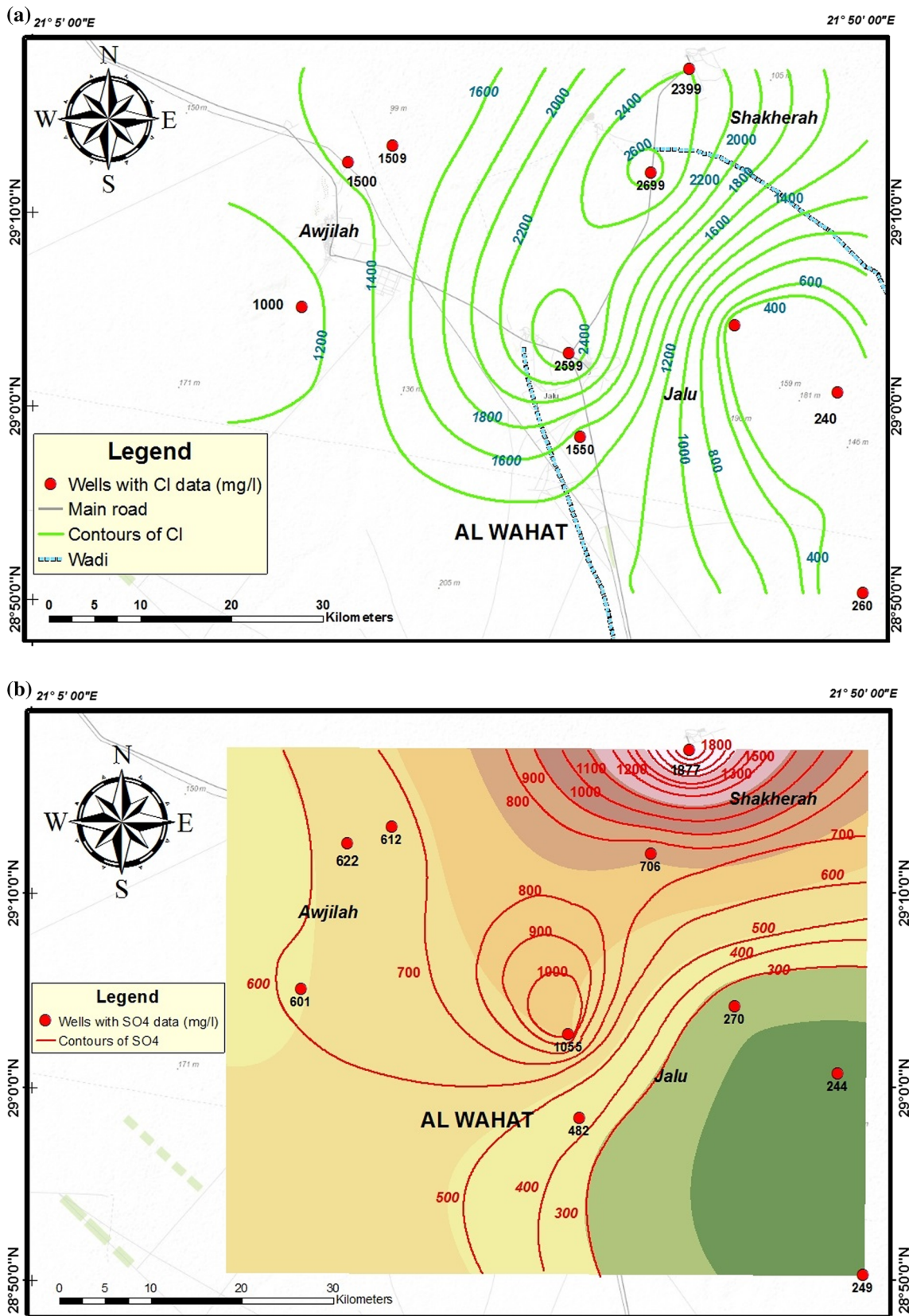
Fig. 8 **a** Spatial distribution of groundwater Cl^- in Al Wahat. **b** Spatial distribution of groundwater SO_4^{2-} in Al Wahat

Saturation indices

The saturation indices (SI) for calcite, aragonite, dolomite, anhydrite, gypsum and halite anhydrite were calculated to verify tendency of precipitation and dissolution of these minerals. The selected minerals were based on the major ions in groundwater from the study area. Figure 12 is a diagram showing SI values for calcite, aragonite, dolomite, anhydrite, gypsum and halite. In general, most of the analysed samples are close to saturation (SI mostly close to

Fig. 9 Diagram of ionic delta (ΔSO_4^{2-}) for all analysed samples

0) with respect to calcite ($CaCO_3$), aragonite and dolomite ($MgCa(CO_3)_2$). Only sample S3 seems to be oversaturated (SI > 0), this supersaturation in S3 with respect to calcite and dolomite probably rather points to water in equilibrium with those minerals. During sampling, often dissolved CO_2 gas escapes, slightly raising pH and thus shifting carbonate equilibrium (more CO_3^{2-}), such that SI > 0 is obtained, whereas in water in the aquifer SI is close to zero.

All groundwater samples in the study area are undersaturated towards gypsum ($CaSO_4 \cdot 2H_2O$), anhydrite ($CaSO_4$) and halite (NaCl). Hence, if these minerals are present, their dissolution will play a role in determining the groundwater composition, especially in systems with limited groundwater flow.
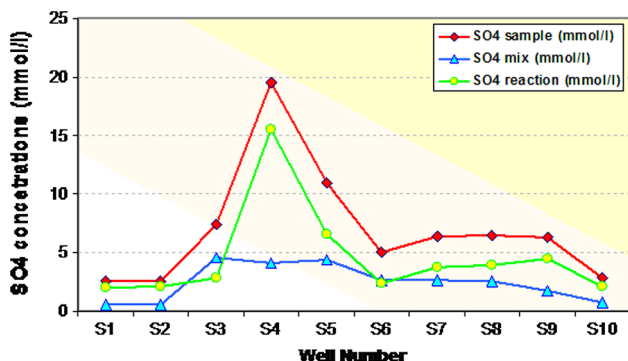
Hydrochemical facies and dissolved ion ratios

Water types according to Piper diagram

Classification of hydrochemical facies for groundwaters according to the Piper diagram is represented in Fig. 13.

In the Piper diagram, almost all water samples from Al Wahat are NaCl type, which generally indicates a strong influence of the marine lithology in the area and upconing
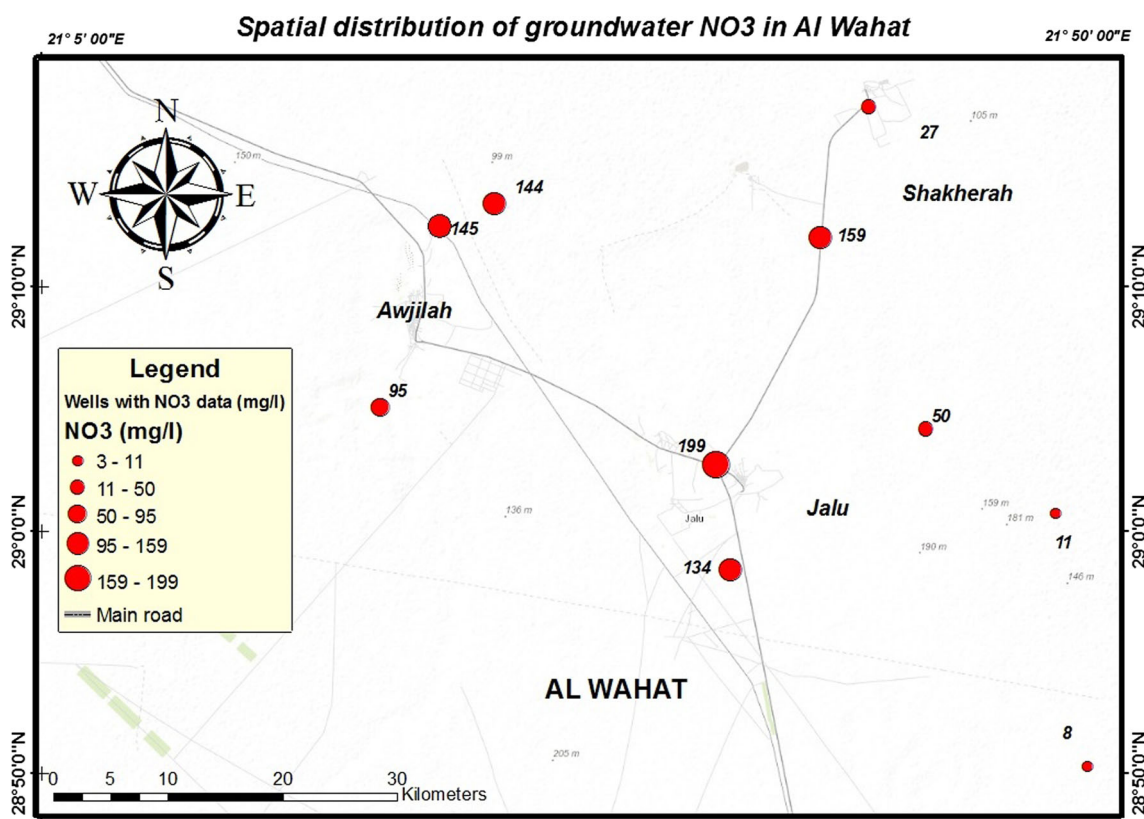
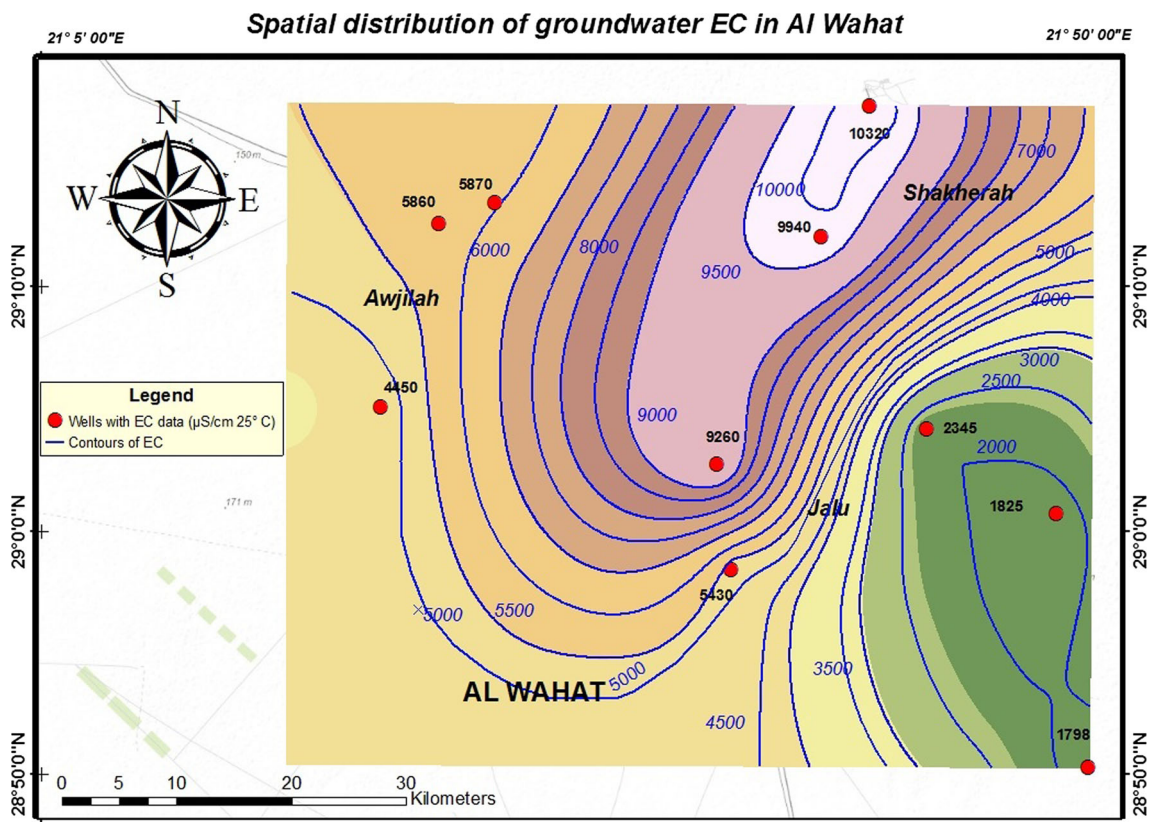**Fig. 10** Spatial distribution of groundwater NO_3^- in Al Wahat

Fig. 11 Spatial distribution of electrical conductivity (EC) in the Post-Eocene aquifer system in Al Wahat

Table 4 Chemical composition of possible end members

Parameter (unit mg/l)	Analysed recharge water in Sarir (sample: SE1)	Analysed recharge water in Tazirbu (sample: W101)	Mediterranean Sea water (Da'as and Walraevens 2010)
pH	8.13	7.48	–
Na^+	56	19	12,700
K^+	23	34	470
Ca^{2+}	32	16	470
Mg^{2+}	19	14	1490
Cl^-	70	13	22,900
SO_4^{2-}	64	11	3190
HCO_3^-	220	189	173
NO_3^-	3	0	0
PO_4^{3-}	0.07	0.01	–
Fe (Total)	0.008	0.001	–
Mn^{2+}	0.01	0.01	–
NH_4^+	0.001	0.001	–
TDS	487	296	41,393

of deep saline water. However, samples from the east and south-east of Jalu Oasis (S1, S2 and S10) are NaMix(HCO_3Cl) type and sample S4 in Shakherah Oasis classified as NaMix($ClSO_4$) type. Furthermore, in the south towards the recharge area in Sarir and Tazerbo, the water type is $NaHCO_3$ and $MgHCO_3$ associated with the lowest
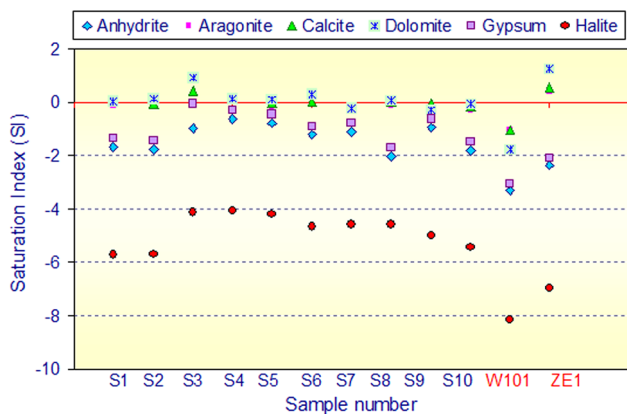
Fig. 12 Calculated saturation indices of groundwater samples with respect to selected minerals

mineralization. This reflects mainly cation exchange reaction during freshening process and the dissolution of carbonate minerals in carbonate aquifers which make up most of the watershed boundaries.

Water-type classification according to Stuyfzand (1986)

Figure 14 shows the spatial distribution of TDS and water types for all samples in Al Wahat. Figure 15 shows the regional groundwater-type distribution in the Post-Eocene aquifer along the flow path in Sirte Basin. Figure 16 shows a hydrochemical cross section in Sirte Basin NE Libya, and the location of the cross section is indicated in Fig. 2 (cross section C–C″).

According to Stuyfzand (1993), the water types in Al Wahat are extremely hard brackish-saline NaCl in the north and east and hard fresh-brackish NaHCO₃ for samples
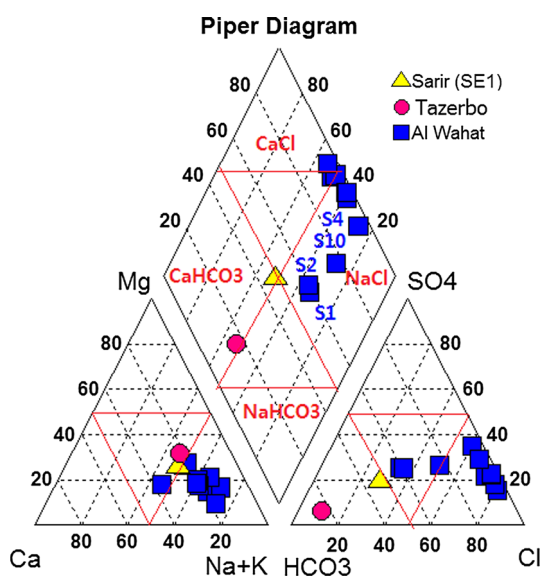

Fig. 13 Water types according to Piper diagram

south-east of Jalu. Only one well (S9) is classified as brackish CaCl water type (the Ca^{2+} is slightly higher than Na^+); however, the (0) indicates equilibrium in the cation exchange.

From Figs. 14, 15 and 16, the following conceptual model can be developed: the groundwaters from the topographic high areas in the south were pushed to the north, in the direction of groundwater movement in the aquifer. The groundwater quality distribution in the Post-Eocene Aquifer results from this evolution, whereby marine conditions are being expelled by the flowing fresh recharge water from the south towards the oases. In the south at the recharge area, the water of the 108 studied wells from Tazerbo Wellfield is mostly $MgHCO_3$ just a few kilometres north of Al Kufra and about 500 km from Al Wahat (Fig. 15). Farther northwards from Tazerbo, the groundwater becomes $NaHCO_3$ type. Downstream in Sarir at about 200 km from Al Wahat, the groundwater is also low mineralized and water type is $NaHCO_3$. Downward flow in Al Wahat (to the south of the Jalu Oasis), the $NaHCO_3$ type still appears and the TDS is more than 1400 mg/l. More towards the north, the NaMix (HCO_3Cl) type is found in Jalu for samples S1, S2 and S10 (TDS < 1500 mg/l), and further northwards the NaCl type is recorded for all samples in Shakherah and Awjilah with higher water mineralization (TDS > 2500 mg/l). In the meantime, salinity increases towards the north, from fresh (F), fresh-brackish (Fb), brackish (B) to brackish-saline (Bs), where the TDS is more than 5000 mg/l in Shakherah and more than 2500 mg/l in Awjilah.

Thus, in an upstream direction, progressively more freshened water types are found. The positive sign (+) found in the upstream direction indicates refreshing takes place, and the (0) sign found in all samples from Awjilah and sample S6 in Jalu indicates cation exchange equilibrium. Sampling points in the north belong to the brackish and brackish-saline major type ($Cl^- > 300$ mg/l) and are very hard to extremely hard due to strong influence of marine lithology and pumping (with cation exchange code "−"or "0"). Samples from the south are fresh to fresh-brackish and moderately hard to hard with (+) cation exchange code indicating aquifer freshening.

The chromatographic sequence of cation exchange is expressed by the subsequent surplus of Na^+, followed by K^+ and finally Mg^{2+}, resulting in the $NaHCO_3$ in Al Wahat and $MgHCO_3$ water-type upstream. The sequence of groundwater types observed in the Post-Eocene Aquifer is in excellent agreement with the pattern of natural groundwater flow (see Fig. 3). Although recent groundwater exploitation has to some extent altered the flow pattern in the aquifer (Fig. 6), the regional distribution of groundwater chemistry is still reflecting the natural flow system.

According to Wright et al. (1974), in a significant volume of water in the Post-Eocene aquifer in Sirte Basin, south of 28°N, the TDSs are below 2000 mg/l between 20°E and 22°E and north of 29°, there is a marked increase in salinity which is related both to the marine character of the aquifer and to the mixing by much attenuated water from the deeper part.

There are no detailed recent studies about the hydrochemistry of the Post-Eocene aquifer. This study comes in agreement with the study done by Wright et al. (1974), but the salinity, especially in the north part of Al Wahat, is getting higher. In 1974, the water quality to the south-east of Jalu at wells S1 and S2 showed TDS less than 500 mg/l; the recorded salinity in this study for these wells is more than 1400 mg/l due to high abstraction and mixing with diluted saline water from the deeper aquifer which has poor water quality.

Dissolved ion ratios

Figure 17 shows scatter plots of TDS versus Cl^-, Cl^- versus Na^+, Cl^- versus SO_4^{2-} and TDS versus NO_3^-. The upstream direction of the upper aquifer in the region is accompanied by a general increase in Na^+, Mg^{2+} and

Fig. 15 Regional groundwater quality distribution in the Post-Eocene ▶ aquifer in NE Libya. Water-type codes are according to the classification system of Stuyfzand (1986, 1993)

HCO_3^-, where HCO_3^- and Na^+ become dominant. As mentioned above, towards the south of the oases, the fresh-brackish hard $NaHCO_3$ type is found, related to cation exchange reaction during freshening of the aquifer. A positive increase in Cl^- concentration with increasing TDS is observed ($r = 0.97$, Fig. 17a). This can also be seen in the plots of Na^+ versus Cl^- ($r = 0.93$) and Cl^- versus SO_4^{2-} ($r = 0.81$). In Fig. 17b, Na^+ and Cl^- also correlate positively and significantly ($r = 0.93$), which can be explained by marine origin of the sediments and mixing with deep saline water. The relation in Cl^- versus SO_4^{2-} graph (Fig. 17c) also reflects the marine nature of the aquifer sediments.

The scatter diagram in Fig. 16d shows high NO_3^- concentrations for many samples in the oases and they correlate positively with TDS ($r = 0.60$). Elevated nitrate concentrations can be attributed to either the disposal of untreated sewage water from disposal ponds and septic tanks or the infiltration of irrigation water saturated with
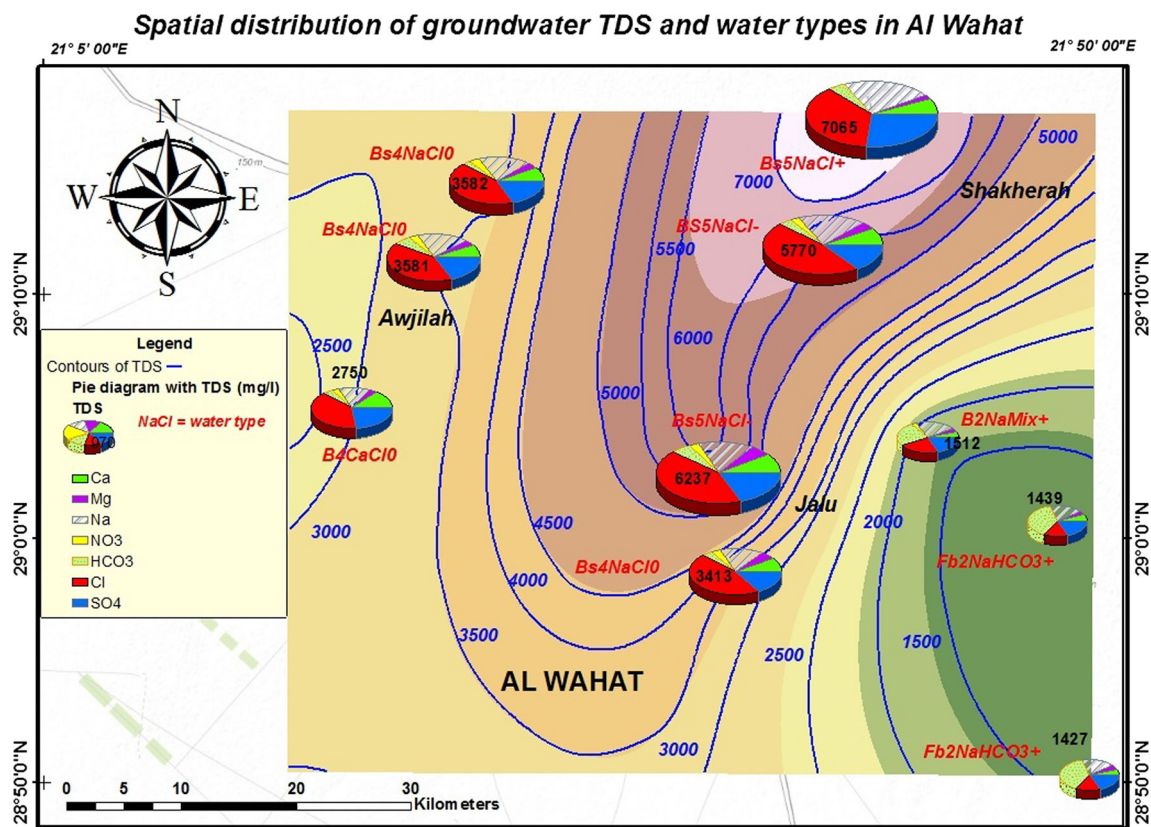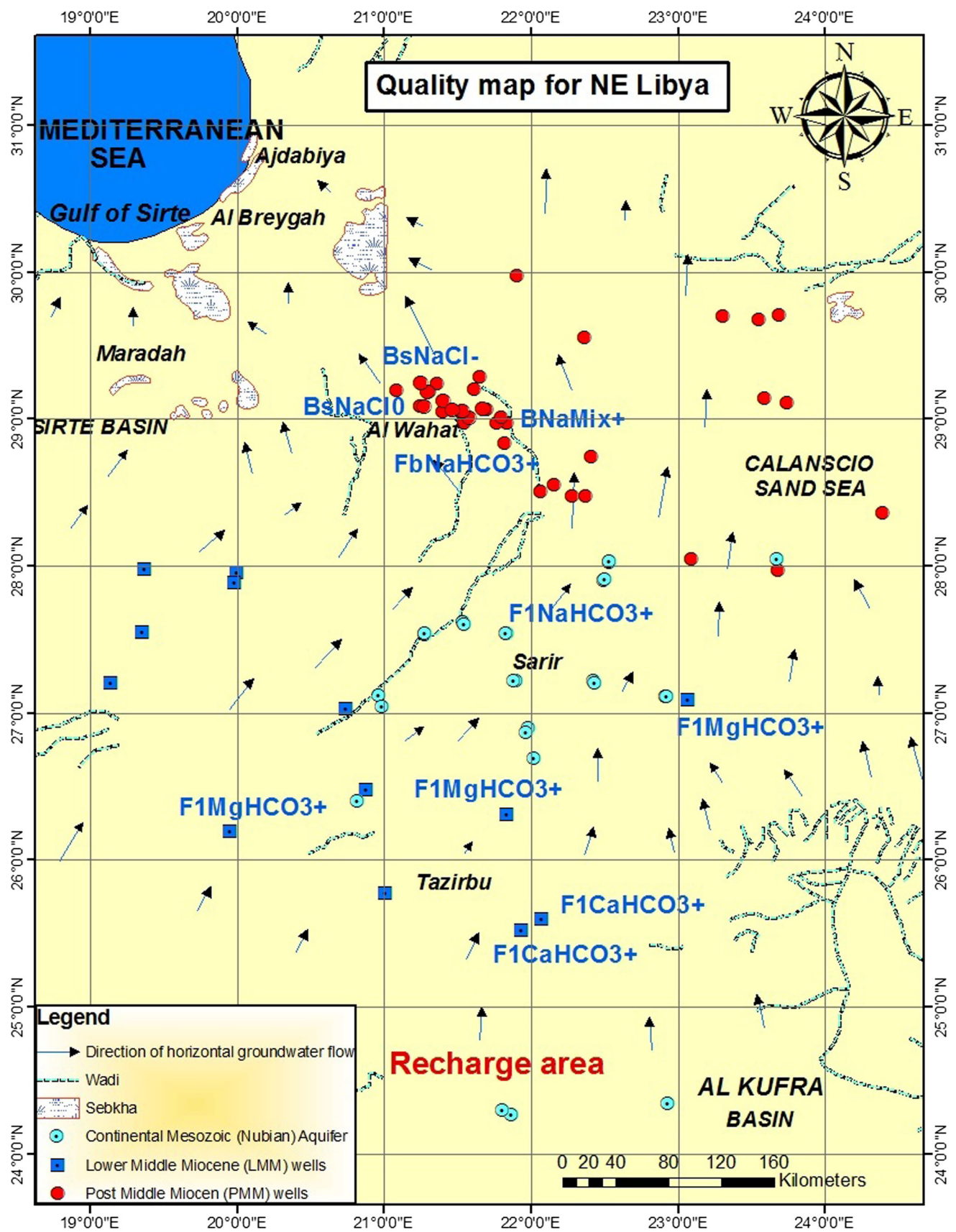

Fig. 14 Spatial distribution of TDS (mg/l) and groundwater types in Al Wahat
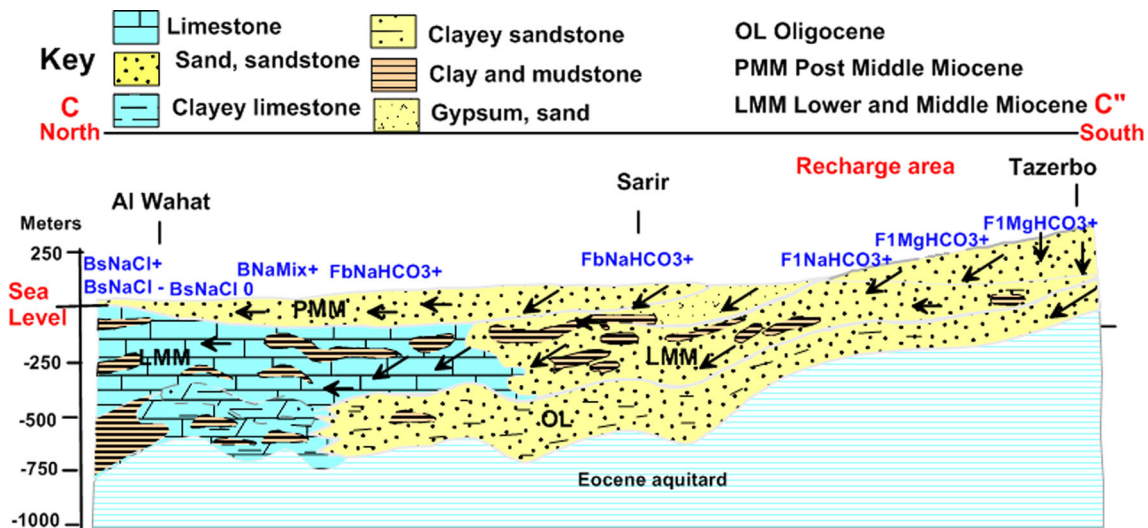
Quality map for NE Libya

Fig. 16 Hydrochemical cross section in NE Libya (cross section C–C″ in Fig. 2)

fertilizing chemicals. In the north of Al Wahat, there are more effects of the marine environment and the aquifer is highly abstracted for irrigation, and as a consequence, higher TDS and high NO_3^- are recorded.

Figure 18a, b shows the ion ratio diagrams (Na^+/Cl^- vs. Cl^- and SO_4^{2-}/Cl^- vs. TDS) based on the analytical results.

Lower ratios of Na^+/Cl^- (meq l^{-1}/meq l^{-1}) than the Mediterranean Sea water ratio (0.88, Fig. 18a) indicate the salinization (wells, S5, S6, S7, S3 and S9), as high pumping from these wells can cause upconing of deep saline water.

The Na^+/Cl^- ratios in the study area range from 0.67 to 2.08. Towards the recharge area, the Na^+/Cl^- ratio is rising gradually, where it reaches more than 1 towards the south of the oases (i.e. S1, S2 and S10), due to flushing of the aquifer with freshwater from the south.

Dissolution of gypsum from the aquifer layers contributes to the high TDS and is reflected in the higher SO_4^{2-}/Cl^- ratio (Fig. 18b), where samples S1 and S2 at the south of the region have much higher SO_4^{2-}/Cl^- ratios than the sea water ratio (0.103). Most of the analysed samples are plotted between the ratio of 0.2–1.0, indicating mixing with the saline end member. Few samples with very high salinity (e.g. S3, S5) are having SO_4^{2-}/Cl^- ratio close to the Mediterranean Sea value (0.103).

Conclusion

Freshening of marine sediments has been studied for Al Wahat region. The result of the study shows the control of cation exchange on water quality in the Post-Eocene Aquifer. The groundwater quality distribution in the aquifer is the result of a spatial separation of the marine cations being sequentially desorbed by the recharging freshwater from the south, revealing a chromatographic pattern. However, in the downstream northern parts of the aquifer where flow is limited due to intensive clay intercalation, cation exchange processes are less effective and only slow gradual dilution of stationary fossil sea water occurs. The synsedimentary marine influence plays an important role in the aquifer hydrochemistry. The sequence of groundwater types observed in the Post-Eocene Aquifer is in excellent agreement with the pattern of natural groundwater flow. The chromatographic sequence of cation exchange is expressed by the subsequent surplus of Na^+, followed by K^+ and finally Mg^{2+}, resulting in the $NaHCO_3$ water type in Al Wahat and $MgHCO_3$ water-type upstream, expressing increasing freshening in the upstream direction.

Hydrogeochemical facies of NaCl type and enrichment of Na^+ and Cl^- can also be attributed to upconing of deep saline water where deeper, less freshened water types are moving upward as a result of aquifer overabstraction. The dissolution of evaporites from the aquifer sediments may play also an important role in the aquifer hydrochemistry, where concentrations of SO_4^{2-} rise to >1000 mg/l. High levels of NO_3^- concentration result from the infiltration of irrigation water and urban untreated wastewaters which are partially responsible for the groundwater quality degradation.

In conclusion, the water quality distribution and chemical characteristics in Al Wahat have been shaped
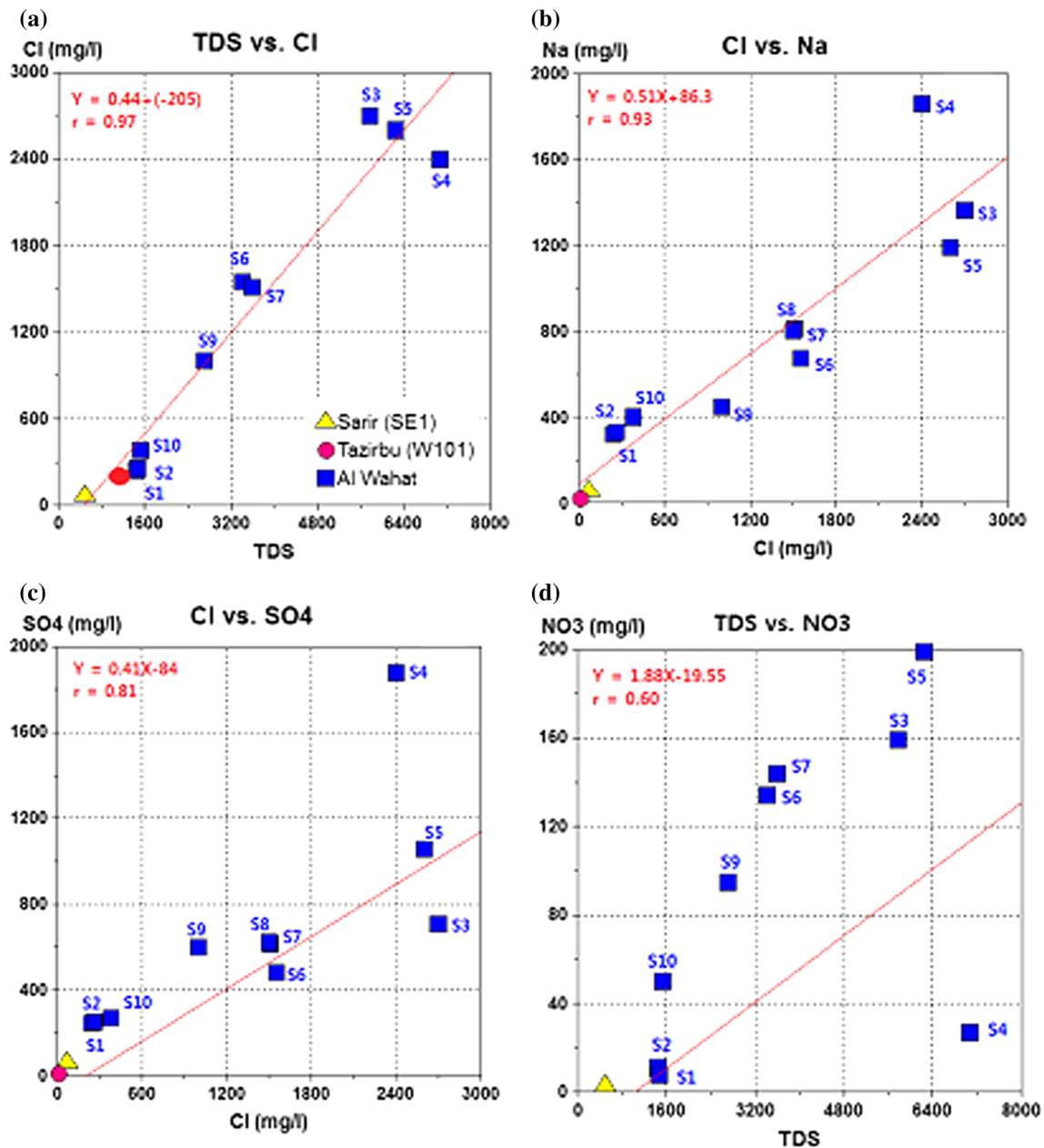
Fig. 17 TDS versus Cl, Cl versus Na, Cl versus SO$_4$ and TDS versus NO$_3$. The *lines* represent a linear regression

by important factors: lithological controls and the marine nature of the sediments, anthropogenic pollution and upconing of deep salt water under pumping wells.

Several chemical parameters of groundwater samples were not within the WHO (2008) guidelines for drinking water, rendering the water non-suitable for human consumption. Therefore, understanding the origin and mechanisms of the salinization process is essential for preventing further deterioration of groundwater resources

in the study area, and more detailed hydrochemical investigations with more water quality data have to be carried out in the region. The main source for high nitrate concentrations has to be identified, and therefore, isotopic analysis is recommended.

This study is an example providing general understanding for the aquifers hydrochemistry in this arid region, by identifying relevant end members and chemical reactions.
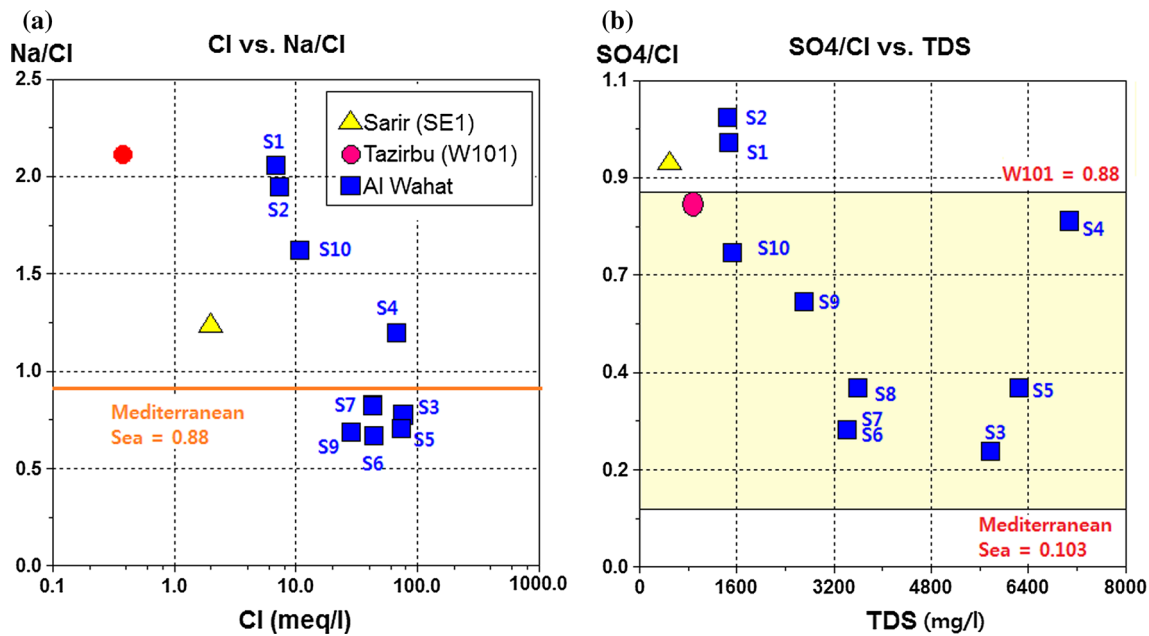
Fig. 18 a Molar ratio of Na/Cl versus Cl^- concentrations. **b** Molar ratio of SO_4^{2-}/Cl^- versus TDS concentrations

References

Ahmad MU (1983) A quantitative model to predict safe yield for wellfield in the Kufra and Sarir Basins, Libya. Ground Water 21(1):58–66

Alfarrah N (2011) Hydrogeological and hydrogeochemical investigation of the coastal area of Jifarah Plain, NW Libya. Ph.D. thesis, Laboratory of Applied Geology and Hydrogeology, Ghent University, Belgium

Alfarrah N, Martens K, Walraevens K (2011) Hydrochemistry of the Upper Miocene-Pliocene-Quaternary aquifer complex of Jifarah Plain, NW-Libya. Geol Belgica 14(3–4):159–174

Alfarrah N, Van Camp M, Walraevens K (2013) Deducing transmissivity from specific capacity in the heterogeneous upper aquifer system of Jifarah Plain, NW-Libya. J Afr Earth Sci 85:12–21

Alfarrah N, Hweesh A, Berhane G, Walraevens K (2016) Groundwater quality assessment, hydrochemical characteristics and flow regime of the nubian aquifer system in tazerbo wellfield at the south-east of Libya. Hydrogeol **(submitted)**

Ambrose G (2000) The geology and hydrocarbon habitat of the Sarir Sandstone, SE Sirt Basin, Libya. J Petrol Geol 23(2):165–191

Appelo CAJ (1994) Cation and proton exchange, pH variations, and carbonate reactions in a freshening aquifer. Water Resour Res 30:2793–2805

Appelo CAJ, Postma D (1993) Geochemistry, groundwater and pollution. A.A. Balkema, Brookfield

Appelo CAJ, Willemsen A (1987) Geochemical calculations and observations on salt water intrusions. 1. A combined geochemical/mixing cell model. J Hydrol 94:313–330

Back WW (1966) Hydrochemical facies and ground-water flow patterns in northern part of Atlantic Coastal Plain: U.S. Geological Survey Professional Paper, 498-A

Baird DW, Aburawi RM, Bailey NJL (1996) Geohistory and petroleum in the central Sirt Basin. In: Salem MJ, El-Hawat AS, Sbeta AM (eds) The geology of Sirte Basin, vol 3. Elsevier, Amsterdam, pp 3–56

Ball J (1927) Problems of the Libyan Desert. Geogr J 70(1):21–38

Beekman HE (1991) Ion chromatography of fresh- and seawater intrusion. Ph.D. thesis, Free University, Amsterdam

Blaser PC, Kipfer K, Loosli HH, Walraevens K, Van Camp M, Aeschbach-Hertig M (2010) A 40 ka record of temperature and permafrost conditions in northwestern Europe from noble gases in the Ledo-Paniselian Aquifer, Belgium

Cardenal J, Walraevens K (1994) Chromatographic pattern in a freshening aquifer (Tertiary Ledo-Paniselian aquifer, Flanders-Belgium). Min Mag 58A:146–147

Chapelle FH, Knobel LL (1983) Aqueous geochemistry and exchangeable cation composition of glauconite in the Aquia aquifer, Maryland. Ground Water 21:343–352

Coetsiers M, Walraevens K (2006) Chemical characterization of the Neogene Aquifer, Belgium. Hydrogeol J 14:1556–1568

Da'as A, Walraevens K (2010). Groundwater salinity in Jericho Area, West Bank, Palestine. SWIM-21 Salt Water Intrusion Meeting, Ponta Delgada, San Miguel, Azores, Portugal. In: Proceedings, pp 28–31

De Menocal P, Ortiz J, Guilderson T, Adkins J, Sarnthein M, Baker L, Yarusinsky M (2000) Abrupt onset and termination of the African humid period: rapid climate responses to gradual insolation forcing. Quat Sci Rev 19(1–5):347–361

Elakkari TS (2005) Structural configuration of the sirt basin. ITC, Enschede, Netherlands

Ezzat A (1959) Ecological studies of bottom living Amphipods in the Nozha Hydrodrome. Editing and Publication Section, Extension Department, Egypt

Faitouri M (2013) Isotope and noble gas study of three aquifers in central and eastern Libya. Ph.D. Thesis, Colorado State University, USA

Faitouri M, Sanford WE (2015) Stable and radio-isotope analysis to determine recharge timing and paleoclimate of sandstone aquifers in central and southeast Libya. Hydrogeol J. doi:10.1007/s10040-015-1232-7

Fidelibus MD, Gimenez E, Morell I, Tulipano L (1993) Salinization processes in the Castellon plain aquifer (Spain). In: Custodio and Galofre (eds) Study and modelling of saltwater intrusion into aquifers. 12th Salt water intrusion meeting, Barcelona, Nov 1992. CIHS, CIMNE, Barcelona, pp 267–283

Foster MD (1950) The origin of high sodium bicarbonate waters in the Atlantic and Gulf coastal plains. Geochim Cosmochim Acta 1:33–48

Gabert G, Kleinsorge H, Kreysing K, Venzlaff H (1961) Some results of ground water investigations in the republic of Sudan. In: Symposium of Athens. IASH Publication, number 56, pp 201–213

General Water Authority (GWA) (2006) General water authority. Unpublished report

General Water Authority (GWA) (2014) General water authority. Unpublished report

Gossel W, Ebraheem AM, Wycisk P (2004) A very large scale GIS-based groundwater flow model for the Nubian sandstone aquifer in Eastern Sahara (Egypt, northern Sudan and eastern Libya). Hydrogeol J 12:698–713

Gras R, Thusu B (1998) Trap architecture of the Early Cretaceous Sarir Sandstone in the eastern Sirte Basin, Libya. In: Macgregor SD, Moody JTR, Clark-Lowes DD (eds) Petroleum geology of North Africa: Geological Society (London) Special Publication 132, pp 317–334

Gumati YD, Kanes WH (1985) Early tertiary subsidence and sedimentary facies-Northern Sirte Basin, Libya. Am Assoc Petrol Geol Bull 69:39–52

Gumati YD, Nairn AEM (1991) Tectonic subsidence of the Sirte Basin, Libya. J Petrol Geol 14:93–102

Harding TP (1984) Graben hydrocarbon occurrences and structural style. AAPG Bull 68(3):333–362

Jones BF, Vengosh A, Rosenthal E, Yechieli Y (1999) Geochemical investigations. In: Seawater intrusion in coastal aquifers: concepts, methods, and practices. Kluwer, Dordrecht, The Netherlands, pp 51–71

Kroner A (1993) The Pan-African belt of north-eastern and eastern Africa, Madagascar, southern India, Sri Lanka and east Antarctica; Terrane amalgamation during formation of the Gondwana Supercontinent. In: Thorwiehe U, Schandelmeier H (eds) Geoscientific research in Northeast Africa. A.A. Balkema, Rotterdam, pp 3–9

Lawrence AR, Lloyd JW, Marsh JM (1976) Hydrochemistry and ground-water mixing in part of the lincolnshire limestone aquifer, England. Groundw 14:320–327

Mohamed C, Zineb A (2015) Geochemistry and hydrogeochemical process of groundwater in the Souf valley of Low Septentrional Sahara. Algeria 9(3):261–273

Pallas P (1981) Water Resources of the Socialist People's Libyan Arab Jamahiriya. In: Salem MJ, Busrewil MT (eds) Geology of Libya. Academic Press, London, pp 539–594

Pallas P, Salem O (2000) Water resources utilization and management of the Socialist Peoples Arab Jamahiriya. In: Regional management of aquifer systems in arid zones: managing non-renewable resources. Proceedings of Tripoli Conference, 1999, UNESCO, Paris, pp 147–172

Parkhurst DL, Appelo CAJ (1999) User's guide to PHREEQC (Version 2), A computer program for speciation, batch-reaction, one-dimensional transport, and inverse geochemical calculations. U.S. Geological Survey, USA

Pim R, Binsariti A (1994) The Libyan great man-made river project. Paper 2. The water resource. Proc ICE-Water Maritime Energy 106(2):123–145

Richter BC, Kreitler CW (1993) Geochemical techniques for identifying sources of groundwater salinization. C.K. Smoley, Boca Raton

Salem O, Pallas P (2002) The Nubian Sandstone Aquifer System (NSAS). In: Applegren B (ed) Managing shared aquifer resources in Africa Paris: United Nations Educational, Scientific and Cultural Organization (IHP-VI Series on groundwater 8), pp 19–21

Sandford K (1935) Geological observations on the northwest frontiers of the anglo-Egyptian Sudan and the adjoining part of the southern Libyan Desert. Q J Geol Soc 91(1–4):323–381

Schroter T (1996) Tectonic and sedimentary development of the central Zallah Trough (west Sirt Basin, Libya). In: Salem MJ, Busrewil MT, Misallati AA, Sola MJ (eds) First symposium on the sedimentary basins of Libya, geology of the Sirt Basin, vol 3. Elsevier, Amsterdam, pp 123–136

Sonntag I, Schwarz H, Hirota Y, Henning U (1978) Cell envelope and shape of *Escherichia coli*: multiple mutants missing the outer membrane lipoprotein and other major outer membrane proteins. J Bacteriol 136:280–285

Stuyfzand PJ (1986) A new hydrogeochemical classification of water types: principles and application to the coastal dunes aquifer system of the Netherlands. In: Proceedings 9th Salt Water Intrusion Meeting (SWIM), Delft, The Netherlands, pp 641–656

Stuyfzand PJ (1993) Hydrochemistry and hydrology of the coastal dune area of the western Netherlands. Ph.D. dissertation, Free University (VU), Amsterdam, 90-74741-01-0: 366

Sultan M, Sturchio N, Hassan FA, Hamdan MAR, Mahmood AM, El Alfy Z, Stein T (1997) Precipitation source inferred from stable isotopic composition of Pleistocene groundwater and carbonate deposits in the Western Desert of Egypt. Quat Geol 4:29–37

Van der Meer F, Cloetingh S (1993) Intraplate stresses and subsidence history of the sirte basin (Libya). Tectonophys 226:37–58

Voss CI, Soliman SM (2014) The transboundary non-renewable Nubian Aquifer System of Chad Egypt, Libya and Sudan: classical groundwater questions and parsimonious hydrogeologic analysis and modeling. Hydrogeol J 22:441–468

Walraevens K (1987) Hydrogeology and hydrochemistry of the Ledo-Paniselian in Eastern and Western Flanders (in Dutch). 350 p. + fig. + annexes. Ph.D. Dissertation, Ghent University

Walraevens K (1990) Hydrogeology and hydrochemistry of the Ledo-Paniseliaan semi-confined aquifer in East- and West-Flanders. Academiae Analecta 52, pp 12–66

Walraevens K, Cardenal J (1994) Aquifer recharge and exchangeable cations in a tertiary clay layer (Bartonian clay, Flanders-Belgium). Mineral Mag 58A, pp 955–956

Walraevens K, Van Camp M (2005) Advances in understanding natural groundwater quality controls in coastal aquifers. In: 18 Salt Water Intrusion Meeting (SWIM). Cartagena 2004, Spain, pp 451–460

Walraevens K, Boughriba M, De Breuck W (1993) Groundwater quality evolution in the black–sluice polder area around assenede (Belgium). In: Custodio E, Galofre A (eds) Study and modelling of saltwater intrusion into aquifers. 12th salt water intrusion meeting, Barcelona, Nov 1992. CIHS. CIMNE, Barcelona, pp 121–142

Walraevens K, Cardenal-Escarcena J, Van Camp M (2007) Reaction transport modelling of a freshening aquifer (Tertiary Ledo-Paniselian Aquifer, Flanders-Belgium). Appl Geochem 22:289–305

Walraevens K, Ibrahimu CM, Yohana M, Van Camp M (2015) Sources of salinity and urban pollution in the Quaternary sand aquifers of Dar es Salaam, Tanzania. J Afr Earth Sci 102:149–165

WHO (2008) Guidelines for drinking-water quality (electronic resource): incorporating 1st and 2nd addenda, vol 1, recommendations, 3rd edn. WHO Library Cataloguing-in-Publication Data

Wright EP, Edmunds WM (1971) Hydrogeological studies in central Cyrenaica. Symposium on the geology of libya. University of Libya, Tripoli, pp 459–481

Wright EP et al (1974) Jalu-Tazerbo Project: phase I final report. Institute of geological sciences, London (**unpublished**)

Wright EP, Benfield AC, Edmunds WM, Kitching R (1982) Hydrogeology of the Kufra and Sirte Basins, eastern Libya. Q J Eng Geol 15:83–103

Yüce G (2005) Determination of the recharge area and salinization degree of Karst Springs in the Lamas Basin (Turkey). Isot Environ Health Stud 41(4):391–404